# Strangeness production and the onset of fireball at NA61/SHINE

**1** Onset of deconfinement

**2** Experiment, analysis

**3** Key results

Maciej Lewicki
malewick@cern.ch

# Phases of strongly interacting matter
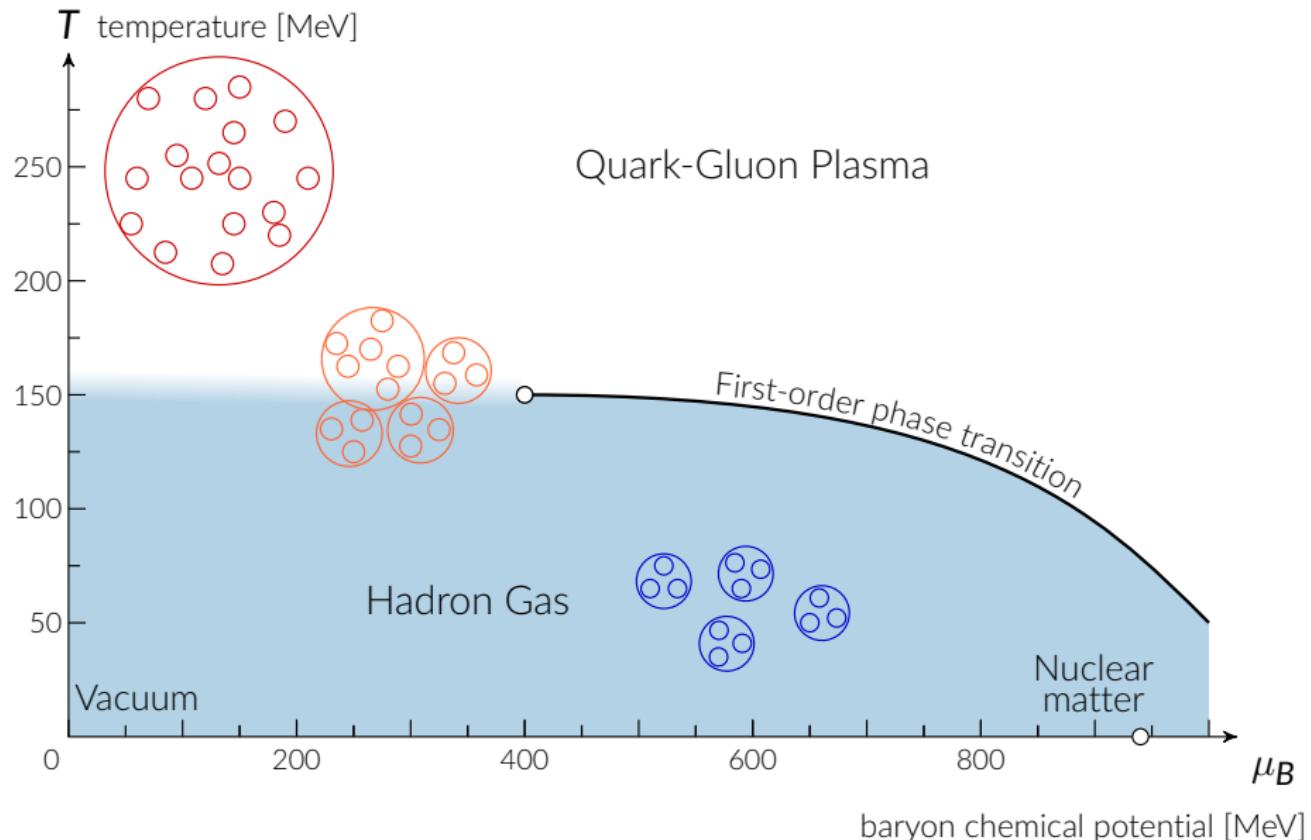
# Phases of strongly interacting matter
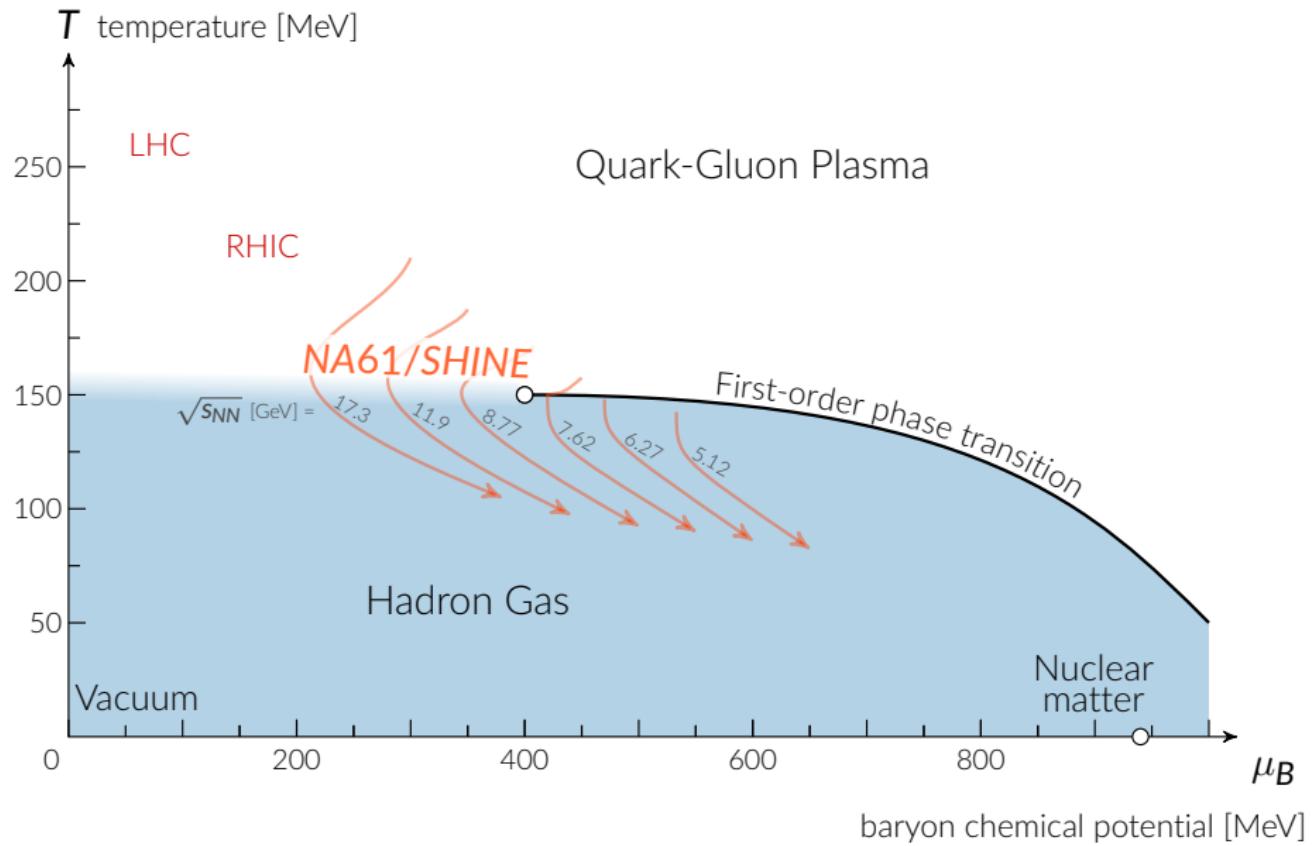
# Signatures of the onset of deconfinement

As predicted in: *Gazdzicki, Gorenstein; Acta Phys.Polon.B 30 (1999) 2705*
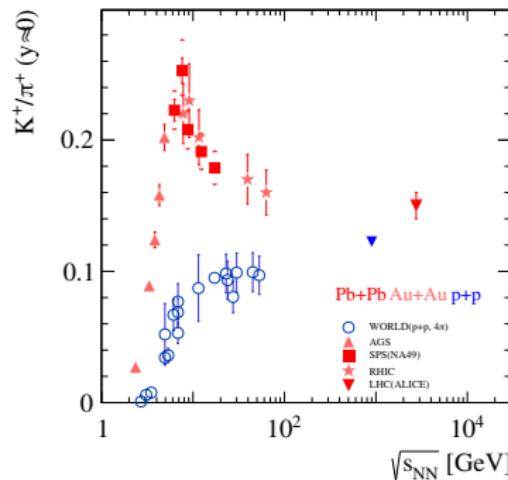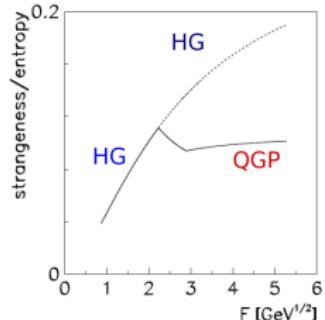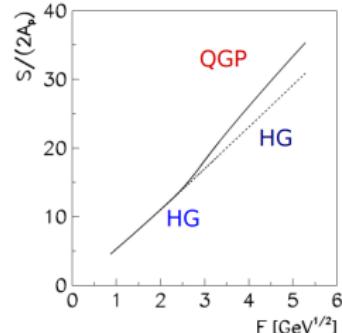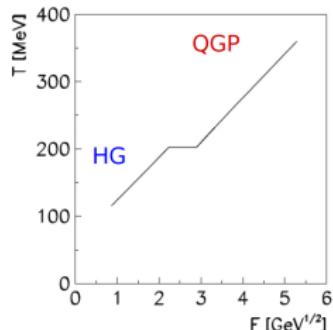


$$F \approx (s_{NN})^{1/4}$$

"horn"

# Strangeness as a probe of deconfinement

- ▶ No strangeness content in colliding nuclei.
- ▶ Sensitive to the state of matter created in the fireball.

|  |  |  |
|---|---|---|
| confined matter | $T_C \approx 150$ MeV | quark-gluon plasma |
| $K$ mesons | $\longrightarrow$ | (anti-)strange quarks |
| $g_K = 4$ | Phase transition | $g_s = 12$ |
| $2M \approx 2 \cdot 500$ MeV |  | $2m \approx 2 \cdot 100$ MeV |

$g_s = 12$ : 2: $q, \bar{q}$, 2×spin, 3×color
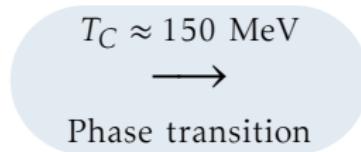
Different numbers of degrees of freedom.

Different masses of strange dof.:

- ▶ relatively heavy kaons ($M > T_C$) in the confined phase,
- ▶ relatively light strange quarks ($m \lesssim T_C$) in QGP.

# Strangeness in Statistical Model of Early Stage

$$\langle n \rangle = \frac{gV}{(2\pi)^3} \int d^3p \frac{1}{e^{E/T} \pm 1}$$

$$\approx gV \left(\frac{MT}{2\pi}\right)^{3/2} e^{-M/T} \quad \text{for heavy particles}$$

$$\approx gV \frac{2\pi^2}{4 \cdot 45} T^3 \quad \text{for light particles}$$
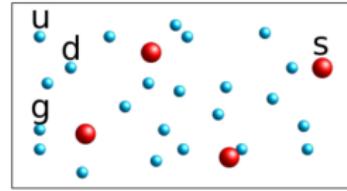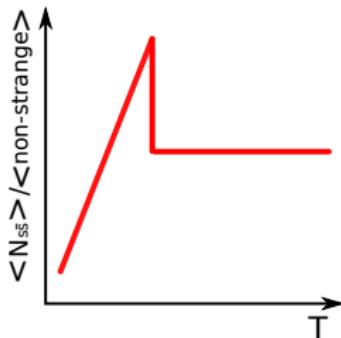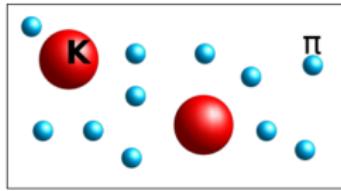


$$\frac{\langle K \rangle}{\langle \pi \rangle} \propto \frac{MT^{3/2}}{T^3} \cdot e^{-M/T}$$

$$\frac{\langle s \rangle}{\langle u + d + g \rangle} \propto \frac{T^3}{T^3} = \text{const}(T)$$

*Gaździcki, Gorenstein, Acta Phys.Polon. B30 (1999) 2705*

# Strangeness in Statistical Model of Early Stage

Temperature dependence
on collision energy in SMES:
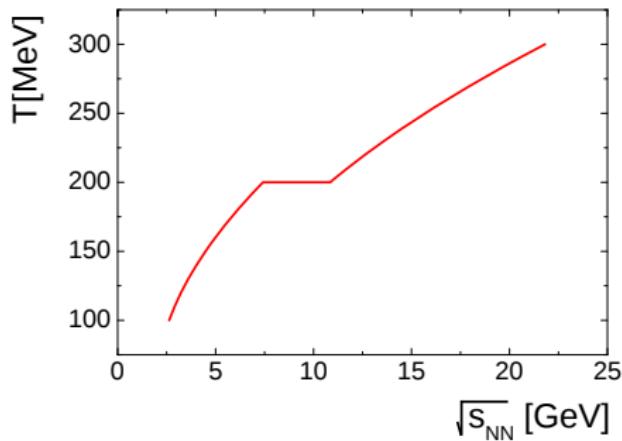
Strange/non-strange
particle ratio:
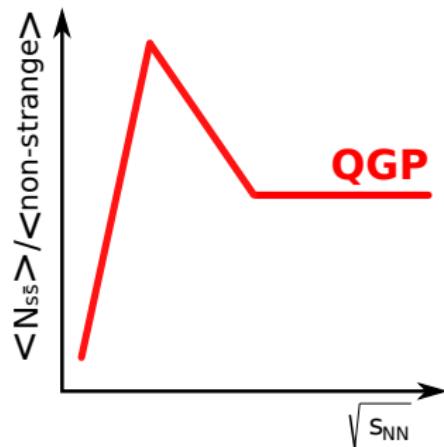


- ▶ Crossing the phase transition leads to a decrease of the strange/non-strange particle ratio – the <u>horn-like structure</u> – Mareks' horn.

# Main strangeness carriers in A+A collisions at high $\mu_B$



$\bar{s}$ $\overset{\text{strangeness}}{\underset{=}{\text{conservation}}}$ $s$

$K^+$ $\overset{\text{isospin}}{\underset{\approx}{\text{symmetry}}}$ $K^0$    $K^-$ $\overset{\text{isospin}}{\underset{\approx}{\text{symmetry}}}$ $\bar{K^0}$

$\overset{\text{high baryon}}{\underset{\text{density}}{\bigvee}}$    $\approxeq$

$\bar{\Lambda}$ $\overset{\text{high baryon}}{\underset{\ll}{\text{density}}}$ $\Lambda$
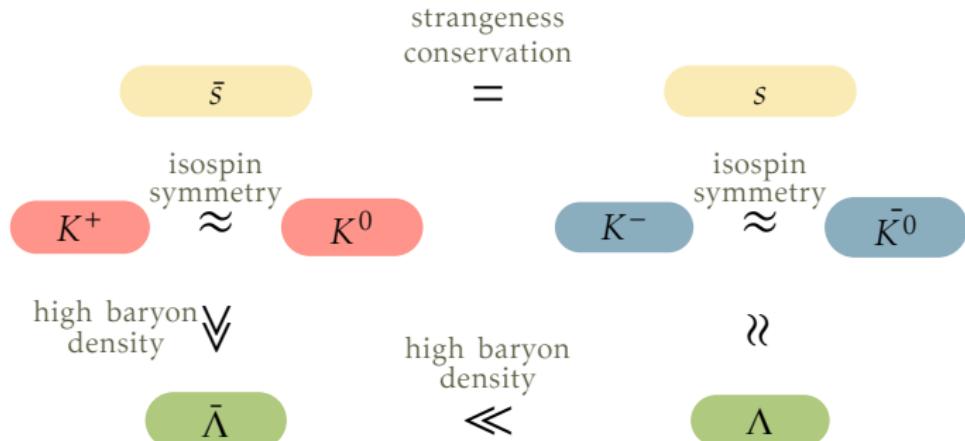
- sensitive to strangeness content <u>only</u>
- sensitive to strangeness content <u>and</u> baryon density

$p + p \;\rightarrow\; p + \Lambda + K^+ + \pi^0$ $\qquad \approx [\text{GeV}]\; 0.94 + 0.94 \rightarrow 0.94 + 1.12 + 0.49 + 0.14$
$p + p \;\rightarrow\; p + p + K^+ + K^-$ $\qquad \approx [\text{GeV}]\; 0.94 + 0.94 \rightarrow 0.94 + 0.94 + 0.49 + 0.49$

The first option is almost 200MeV "cheaper".

# Strange definitions

Strangeness production $\langle N_{s\bar{s}} \rangle$ – number of $s$-$\bar{s}$ pairs produced in a collision.

$$2 \cdot \langle N_{s\bar{s}} \rangle = \langle \Lambda + \bar{\Lambda} \rangle + \langle K + \bar{K} \rangle + \langle \phi \rangle + \dots$$
$$2 \cdot \langle N_{s\bar{s}} \rangle \approx \langle \Lambda \rangle + \langle K^+ + K^- + K^0 + \bar{K}^0 \rangle$$

Entropy production $\propto \langle \pi \rangle$

The experimental ratio of strangeness to entropy can be defined as:

$$E_S = \frac{\langle \Lambda \rangle + \langle K + \bar{K} \rangle}{\langle \pi \rangle} \approx \frac{2 \cdot \langle N_{s\bar{s}} \rangle}{\langle \pi \rangle}$$

$$\langle N_{s\bar{s}} \rangle \approx \langle K^+ \rangle + \langle K^0 \rangle \approx 2 \cdot \langle K^+ \rangle, \qquad \langle \pi \rangle \approx \frac{3}{2} (\langle \pi^+ \rangle + \langle \pi^- \rangle)$$

$$\frac{\langle N_{s\bar{s}} \rangle}{\langle \pi \rangle} \approx \frac{2}{3} \frac{\langle K^+ \rangle}{\langle \pi^+ \rangle}, \qquad E_S \approx \frac{4}{3} \frac{\langle K^+ \rangle}{\langle \pi^+ \rangle}$$

# Canonical suppression of strangeness

- Consider a gas of particles with strangeness $s = +1, 0, -1$ and with total strangeness $S = 0$.
- Thermal density of kaons in (C):

$$n_K = \frac{Z_K^1}{V} \frac{S_1}{\sqrt{S_1 S_{-1}}} \frac{I_1(x_1)}{I_0(x_1)}$$

where

$$Z_K^1 = V \frac{g_K}{2\pi^2} m_K^2 \, T K_2 \left(\frac{m_K}{T}\right)$$

$$S_1 = Z_K^1 + Z_\Lambda^1 + Z_{K^\star}^1 + \dots$$

$$x_1 \equiv 2\sqrt{S_1 S_{-1}} \quad \propto V$$

Volume assumed linear in $N_{part}$:

$$V = \frac{V_0}{2} N_{part}$$

$$F_{CS1} = \frac{I_1(x_1)}{I_0(x_1)}$$
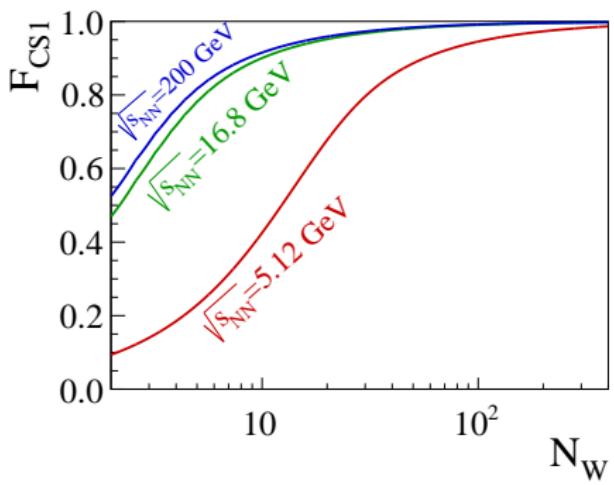
# NA61/SHINE 2D scan
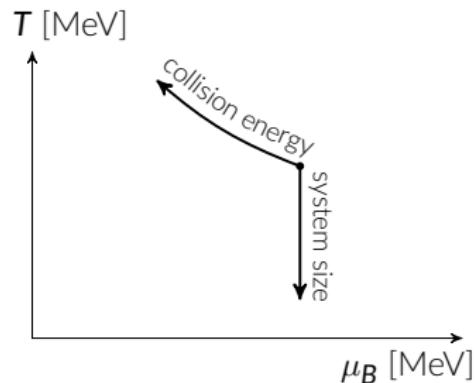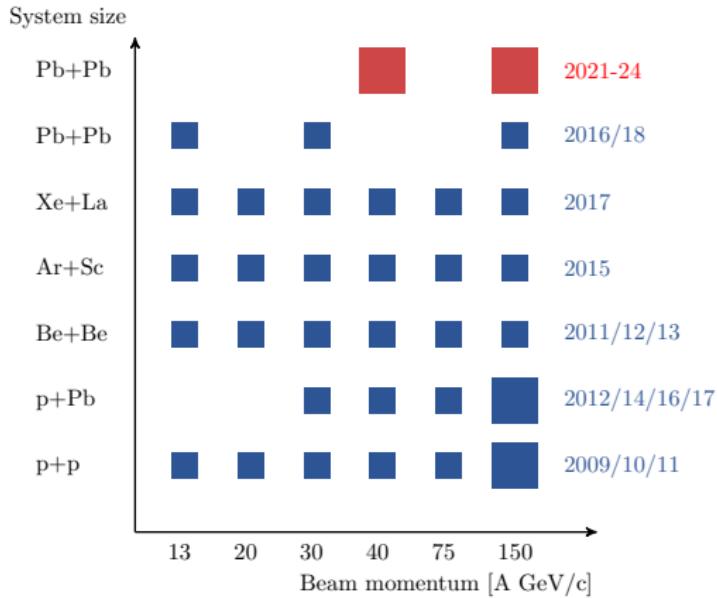


Vovchenko et al.; Phys. Rev. C, 93(6):064906,2016
Becattini et al.; Phys.Rev., C73:044905, 2006

- ▶ Unique, two-dimensional scan in collision energy and nuclear mass number of colliding nuclei.
- ▶ Unique range in the phase diagram of strongly interacting matter.

RUN INFORMATIONS

ID: 53793

RUN NUMBER: 20480

TIME: 2015-02-23T07:58:32Z (UTC)

TAPE NUMBER: 1108713528 (GPS)
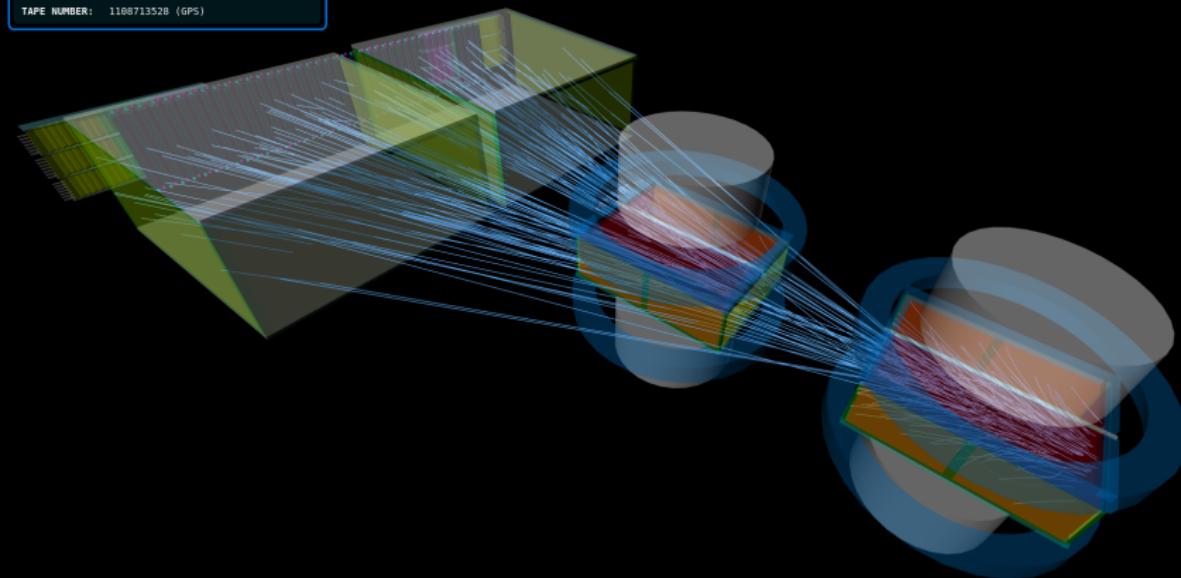
Energy Deposit (dE/dx)

0.5668 1.1327 1.8990 2.2653 2.8317 3.3980 3.9643 4.5307 5.0970 5.6633 6.2296 6.7960 7.3623 7.9286 8.4949 9.0613 9.6276 10.1939 10.7603 11.3266 11.8929 12.4593
1.1326 1.6989 2.2652 2.8316 3.3979 3.9642 4.5306 5.0969 5.6632 6.2295 6.7959 7.3622 7.9285 8.4949 9.0612 9.6275 10.1938 10.7602 11.3265 11.8928 12.4592

© Filip Michalski & Taras Palayda

visualization by: F. Michalski, T. Palayda

Measuring d$E$/d$x$

TPC

charged particle

Landau/Vavilov dE
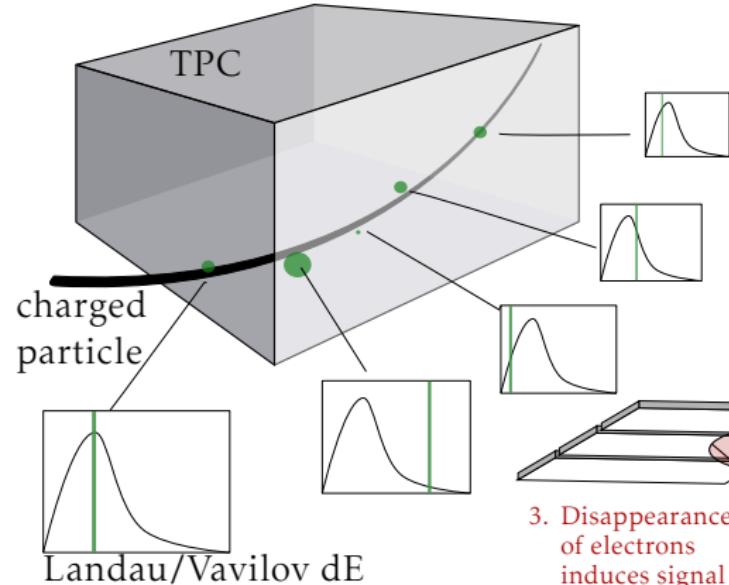
3. Disappearance of electrons induces signal in pad plane

pad plane

Sense wire plane +1kV

Cathode plane

$\vec{E}$

Gating grid

2. Electrons drift in electric field

1. Primary particle ionises gas

charged particle track
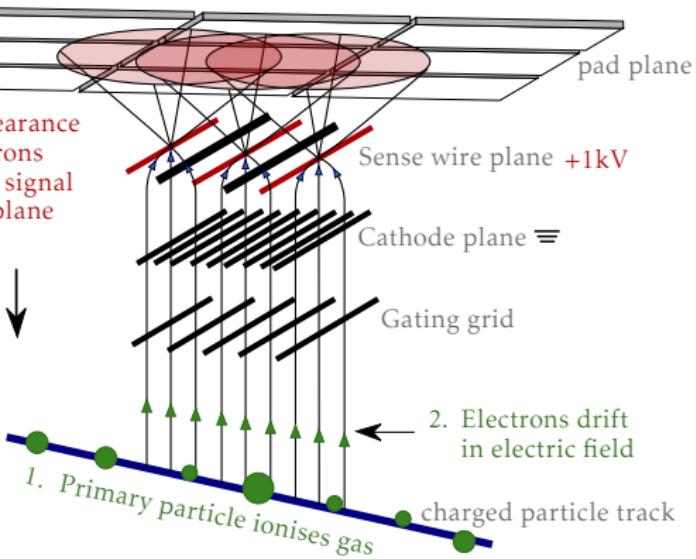
# Particle identification (PID) through d$E$/d$x$
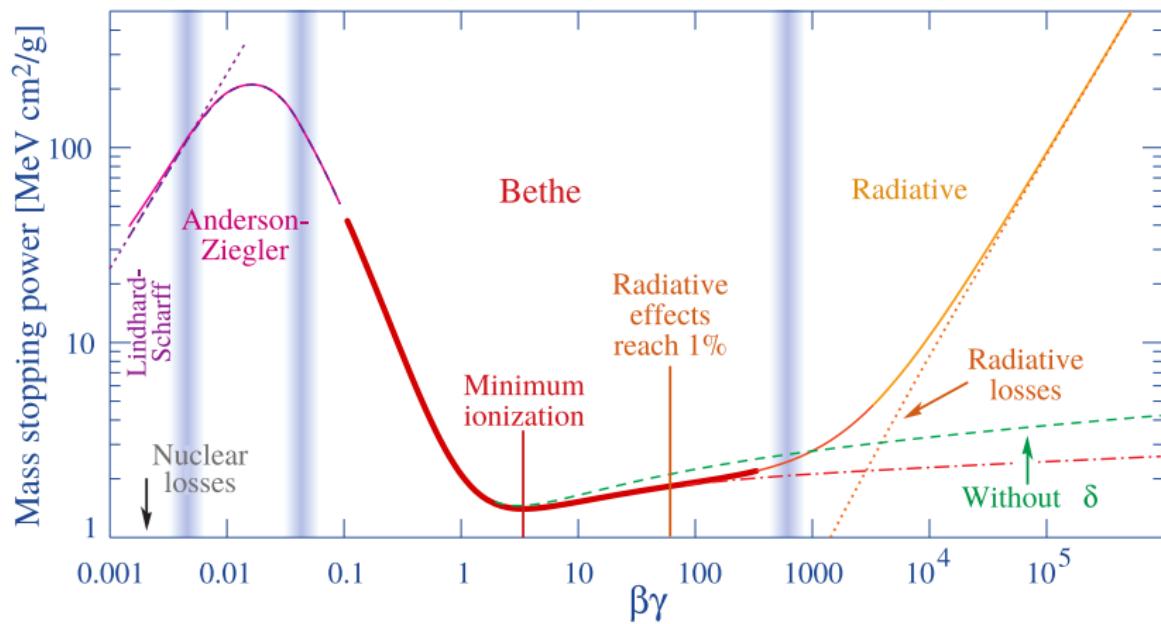


Independent measurements of $p$ and d$E$/d$x$ allows calculation of mass → PID.

# Recorded d$E$/d$x$ vs $p$ distributions
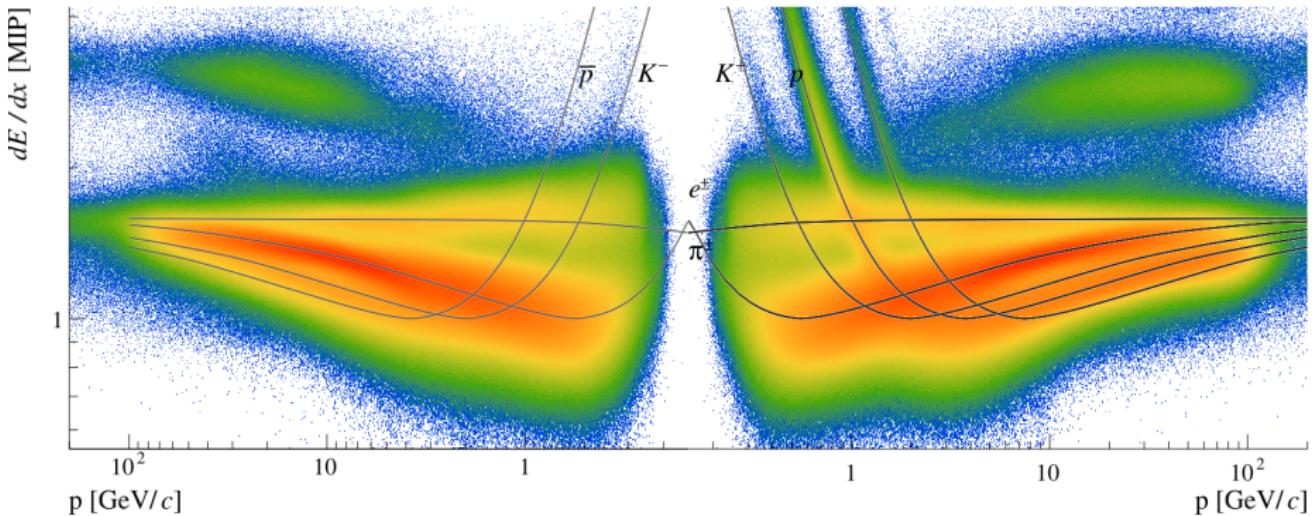


- ▶ Overlap from contributions of different particle species.
- ▶ Contribution of each species needs to be "unfolded".

# Recorded d$E$/d$x$ vs $p$ distributions
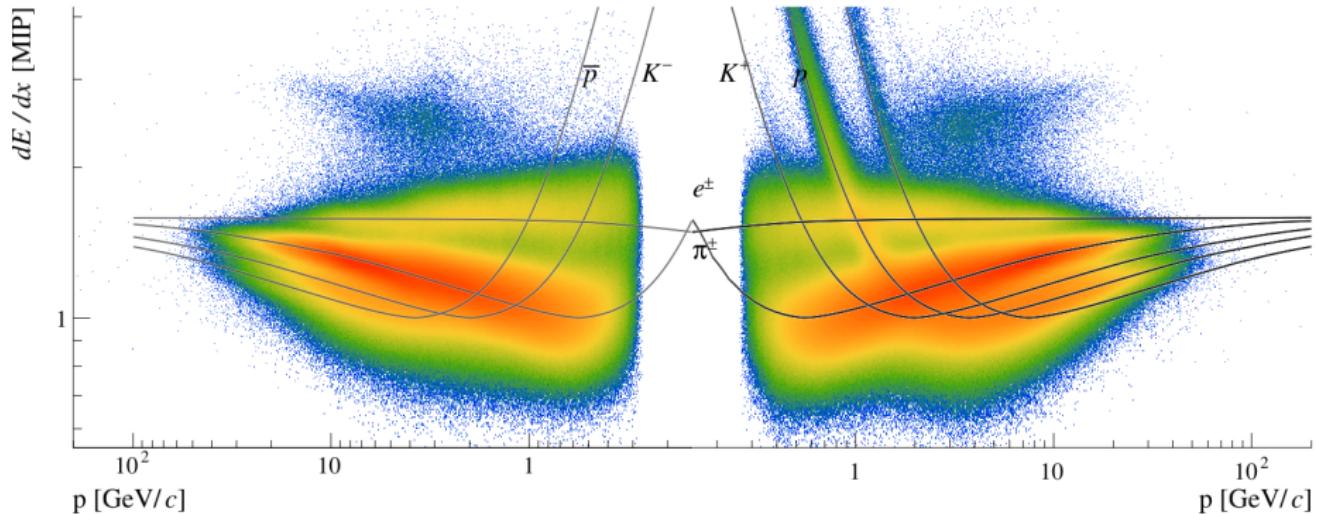


- ▶ Dedicated selection of tracks improves $p$ and d$E$/d$x$ resolution.
- ▶ Here: favourable track topology and required minimal number of points measured in TPCs.

# Recorded d$E$/d$x$ vs $p$ distributions
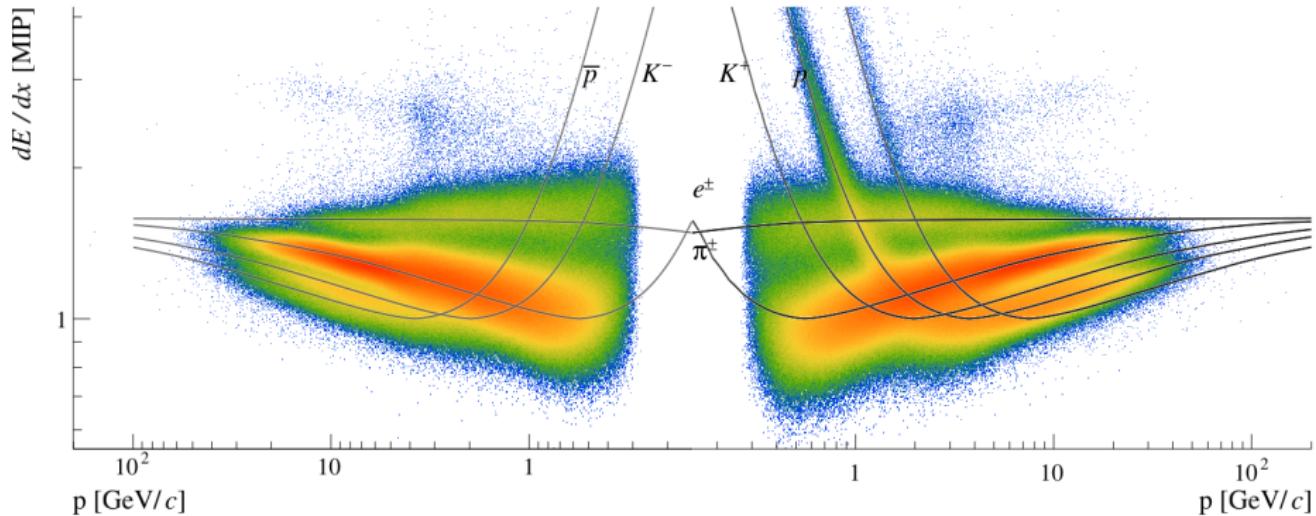


- Additional selection criteria further improve the resolution.
- Selected narrow range of track azimuthal angle at vertex.

# Data binning

Analysis done in bins of $p$ and $p_T$:
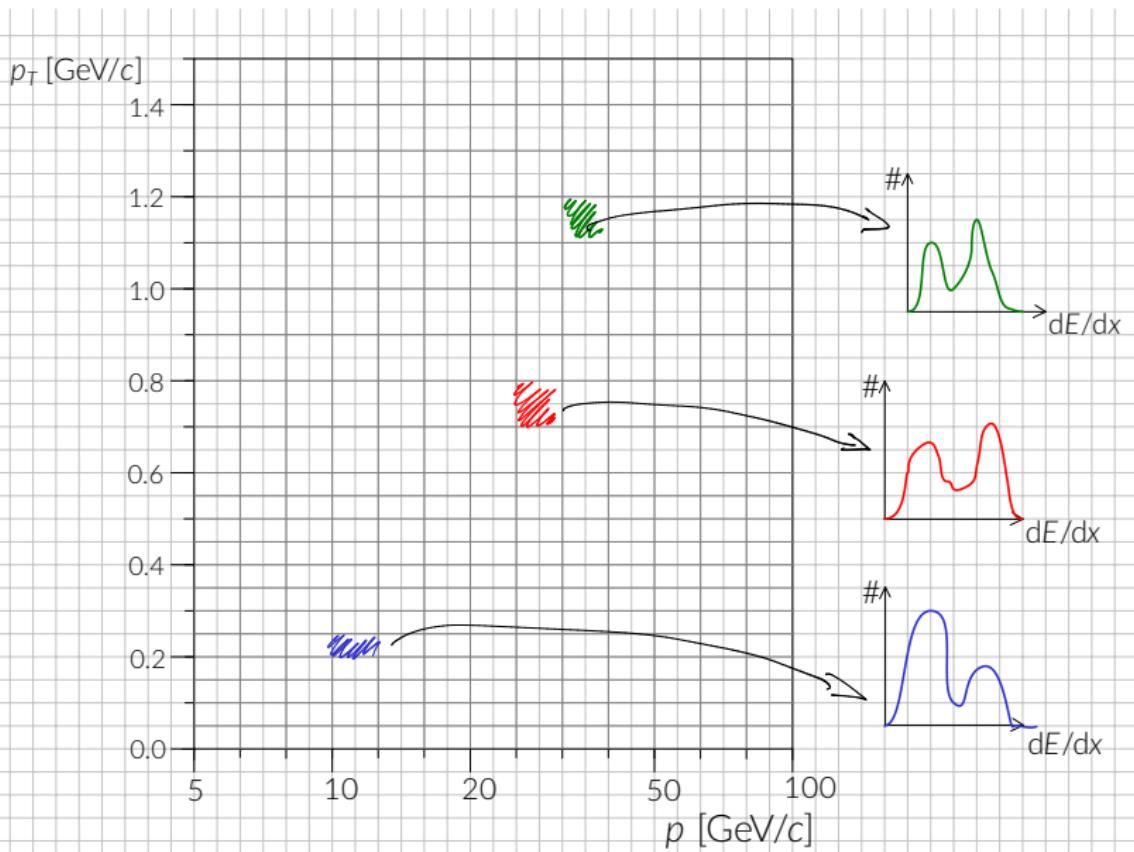
# $dE/dx$ PID
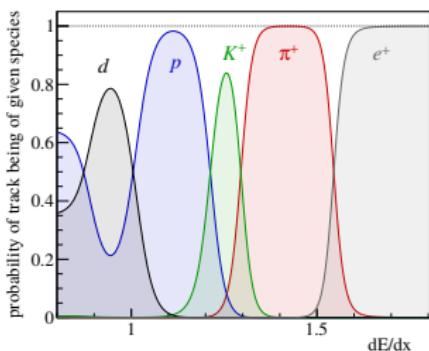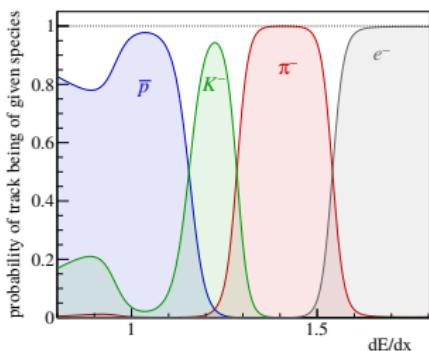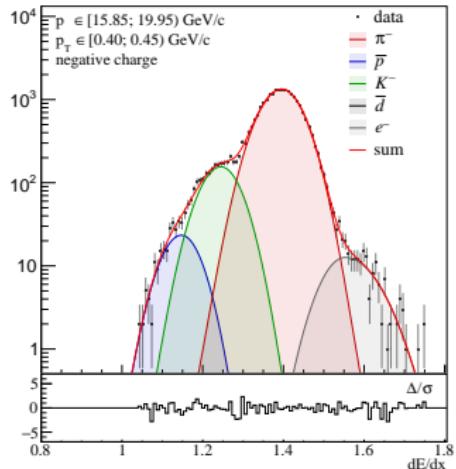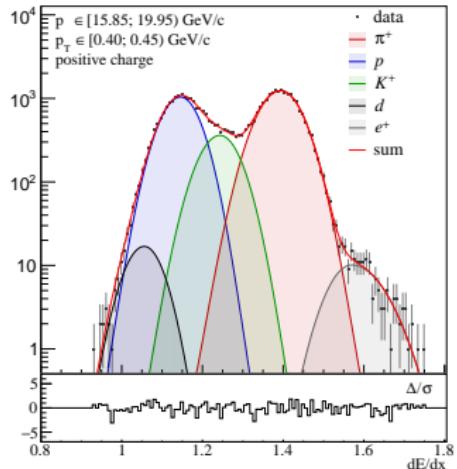
# Simultaneous fit of all $p_T$ bins for given $p$

d$E$/d$x$ p. d. f. (track length weighted):

$$\left\langle \frac{dE}{dx} \right\rangle_{total} = \sum_{i=d,p,K,\pi,e} N_i \frac{1}{\sum_l n_l} \sum_l \frac{n_l}{\sqrt{2\pi}\sigma_{i,l}} \exp\left[ -\frac{1}{2}\left( \frac{x - x_i + \frac{2}{\sqrt{2\pi}}\delta\sigma}{(1 \pm \delta)\,\sigma_{i,l}} \right)^2 \right]$$

with widths $\sigma_{i,l}$
$l \equiv$ # of clusters: $\qquad \sigma_{i,l} = \frac{\sigma_0}{\sqrt{l}}\left( \frac{x_i}{x_\pi} \right)^\alpha \qquad$ and $\qquad \delta = \delta_0/l$

Example:

$$\vec{\theta} = (N_d, N_p, N_K, N_\pi, N_e, \frac{x_d}{x_\pi}, \frac{x_p}{x_\pi}, \frac{x_K}{x_\pi}, x_\pi, x_e, \sigma_0, \delta_0, \alpha)$$

13 parameters (5 amplitudes, 5 positions, width, width scaling and asymmetry)
$\rightarrow$ Impossible to fit without any tricks.

Simultaneous fit of all $p_T$ bins in a given $p_{tot}$ bin.
Shared parameters: $\frac{x_i}{x_\pi}$
Unique parameters: $\sigma_0$, $\delta_0$, $N_i$, $x_\pi$
Fixed parameters: $\alpha$

# Corrections and errors

MC corrections for detector acceptance and inefficiencies using EPOS:

$$n_i^{\text{corrected}} = (n_i^{\text{raw data}} - n_i^{\text{MCrec decay}}) \times \frac{n_i^{\text{MCgen}}}{n_i^{\text{MCrec primary}}}$$

$$n_i \;\rightarrow\; \frac{\mathrm{d}^2 n}{\mathrm{d}y \, \mathrm{d}p_T}$$

- ► Statistical errors calculated with bootstrapping.
- ► Systematic errors calculated by varying any fixed criterion (cuts, fit parameters) imposed on data.

# Identified charged hadrons spectra
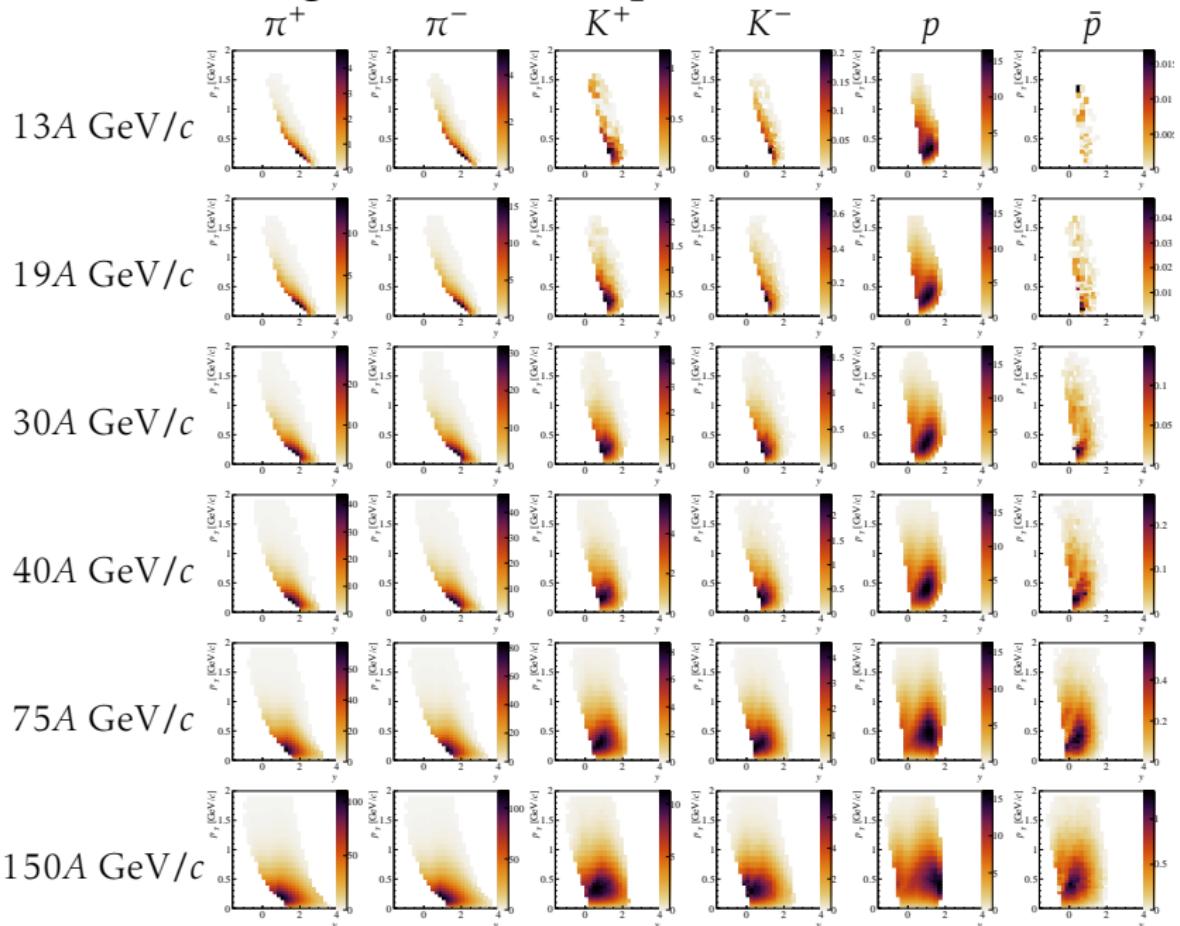
# Supplementary measurements (top: 150*A*, bottom: 30*A* GeV/*c*)

- $dE/dx$:
  $\pi^+, \pi^-, K^+, K^-, p, \bar{p}, (d, \bar{d})$
  at $p \gtrsim 5$ GeV/*c*

- $tof\text{-}dE/dx$:
  $\pi^+, \pi^-, K^+, K^-, p, \bar{p}, (d, \bar{d})$
  at lower momenta

- $h$-minus:
  $\pi^-$ in large acceptance
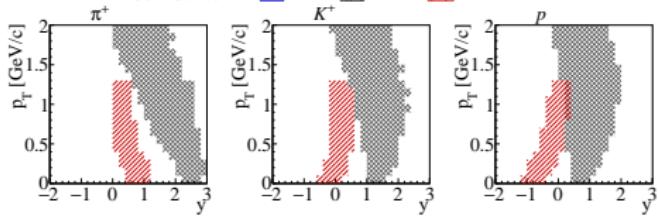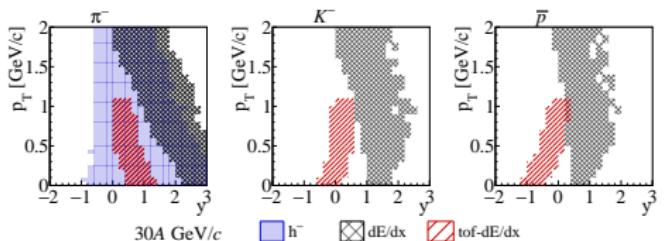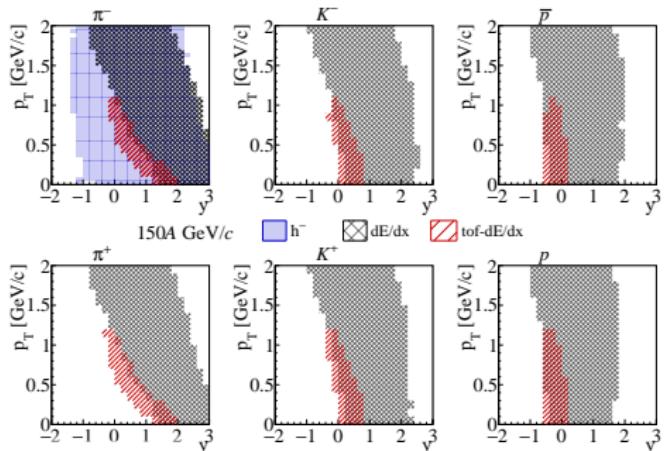
Protons and Antiprotons

# Proton rapidity spectra
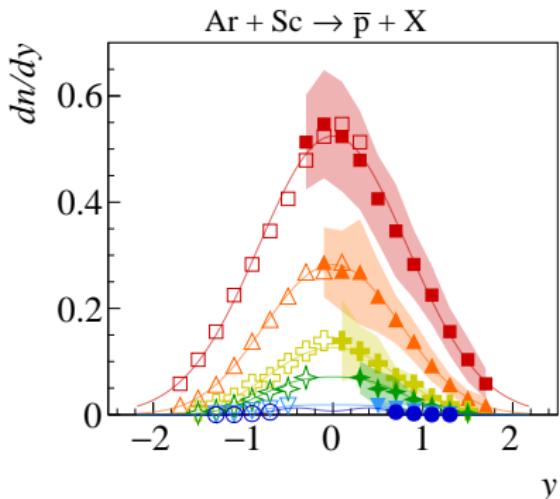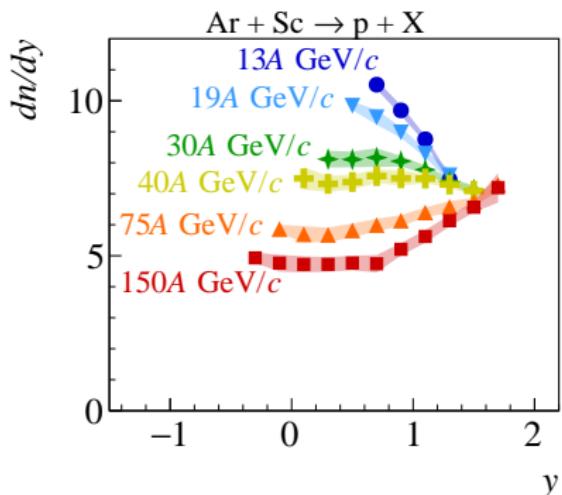


- ▶ Proton and antiproton rapidity spectra were measured.
- ▶ Due to limited acceptance and non-trivial shape of proton spectra mean multiplicities could not be calculated.
- ▶ Antiproton rapidity spectra are well approximated by double-Gaussian fit and mean multiplicities were calculated.

# Proton rapidity spectra for various reactions
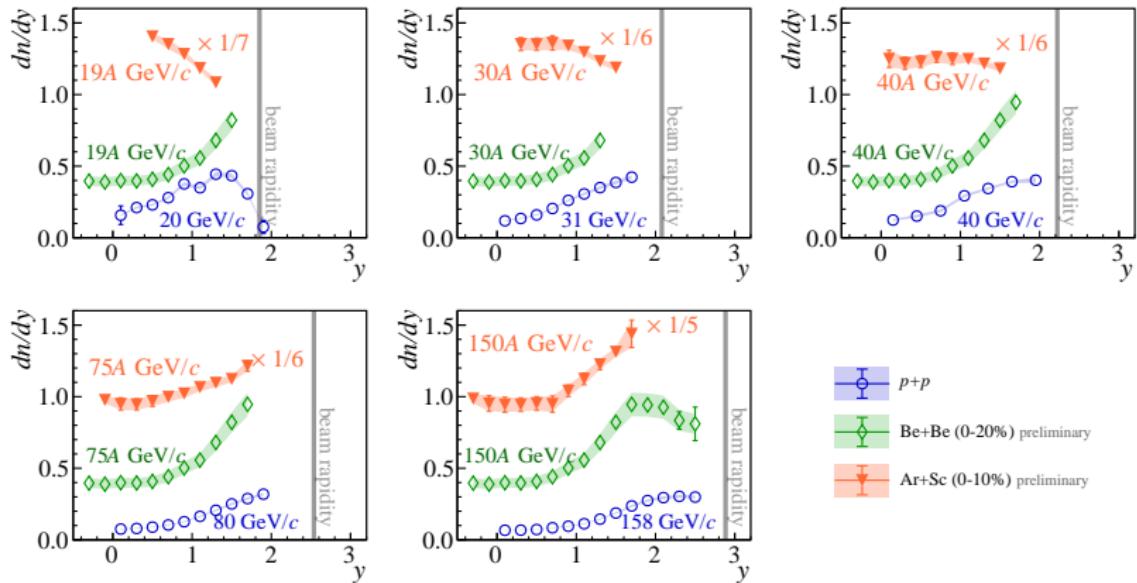


Rapidity spectra measured in Ar+Sc are largely different than the ones measured in small systems.

Charged Kaons

# Extrapolation of measured spectra ($K^+$ example)
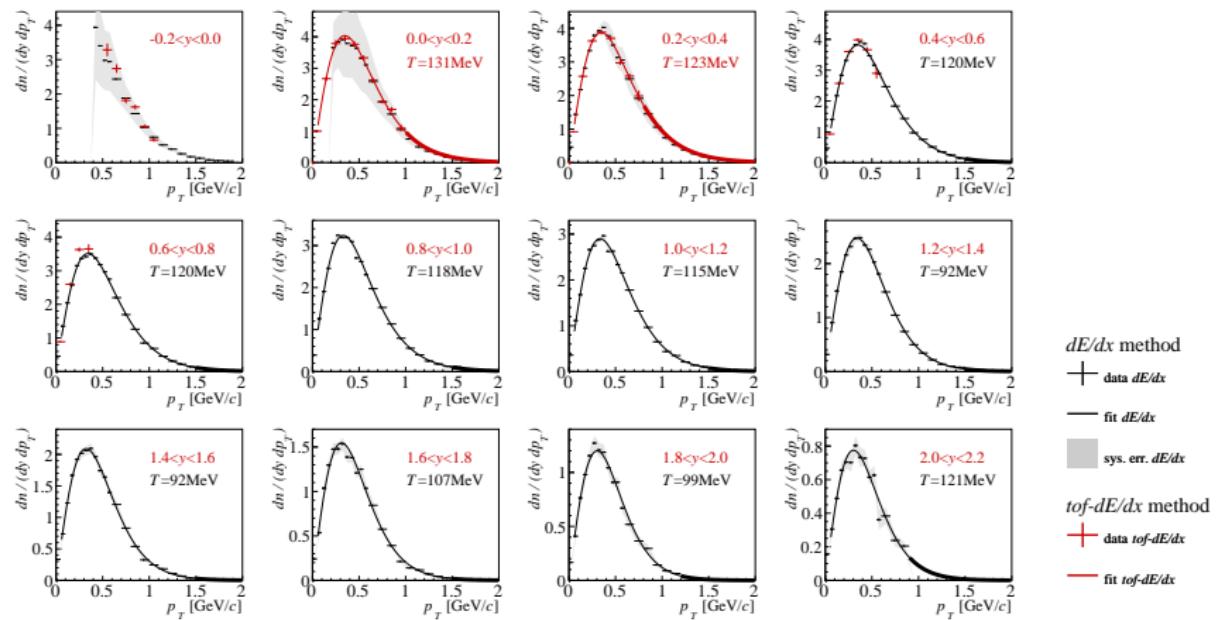


$$\frac{1}{p_T}\frac{d^2}{dp_T \, py} = \frac{A}{T(m_K+T)} \cdot e^{-(m_T-m_K)/T}$$

At each $y$ interval the $dn/dy$ yield is calculated as a sum of measured data and the integral of extrapolated function.

# Kaon rapidity spectra

$Ar + Sc \rightarrow K^+ + X$, $Ar + Sc \rightarrow K^- + X$
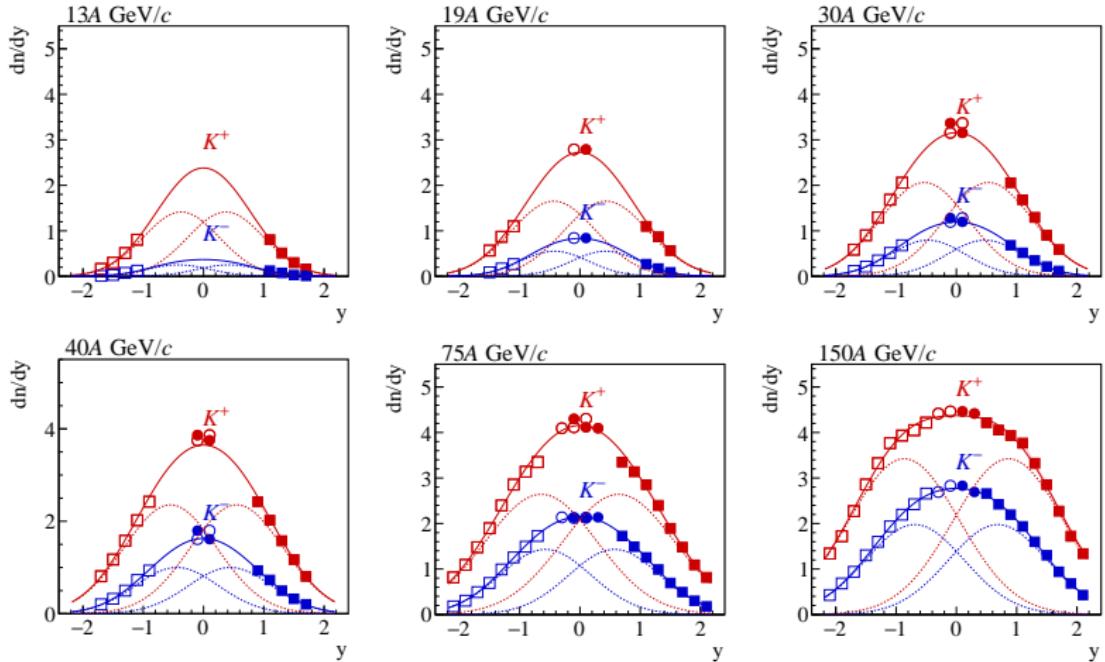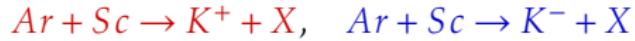


0-10% most central events

$$f_{\text{fit}}(y) = \frac{A}{\sigma_0\sqrt{2\pi}}\exp\left(\frac{-(y-y_0)^2}{2\sigma_0^2}\right) + \frac{A}{\sigma_0\sqrt{2\pi}}\exp\left(\frac{-(y+y_0)^2}{2\sigma_0^2}\right)$$

# System size dependence
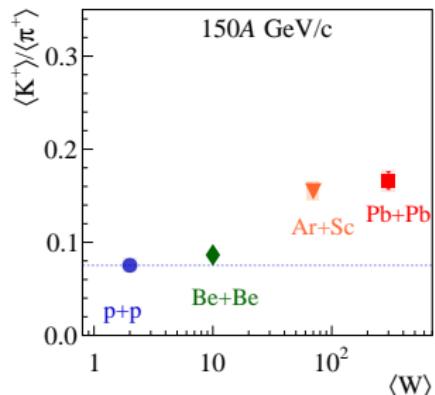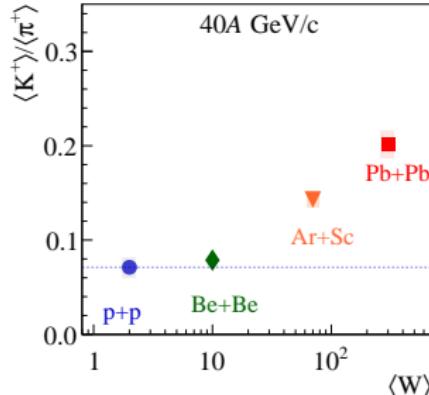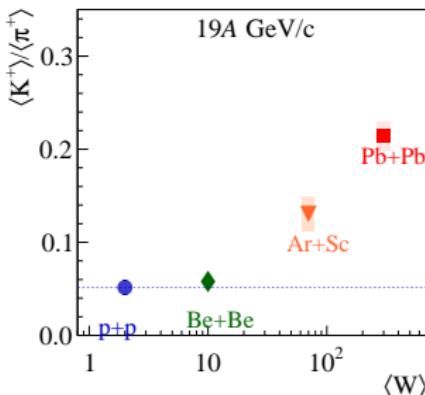


- ▶ At low collision energies Ar+Sc results are placed in between small systems and Pb+Pb.
- ▶ At higher collision energies Ar+Sc measurements approach Pb+Pb.

# Horn – energy dependence of $\langle K^+\rangle/\langle\pi^+\rangle$
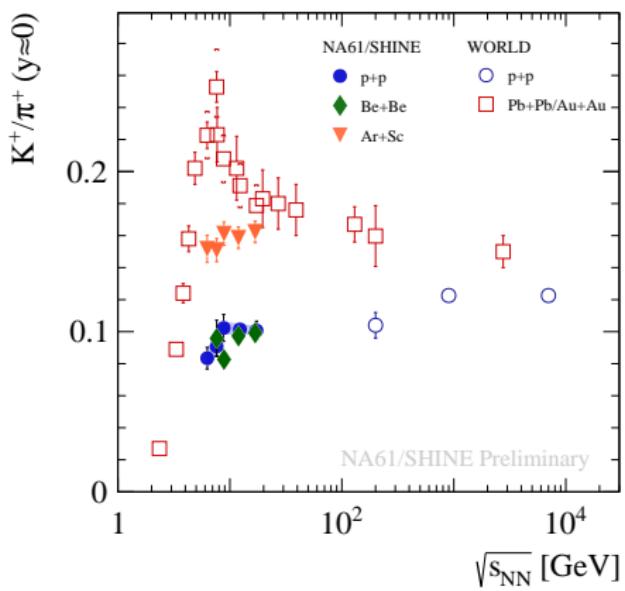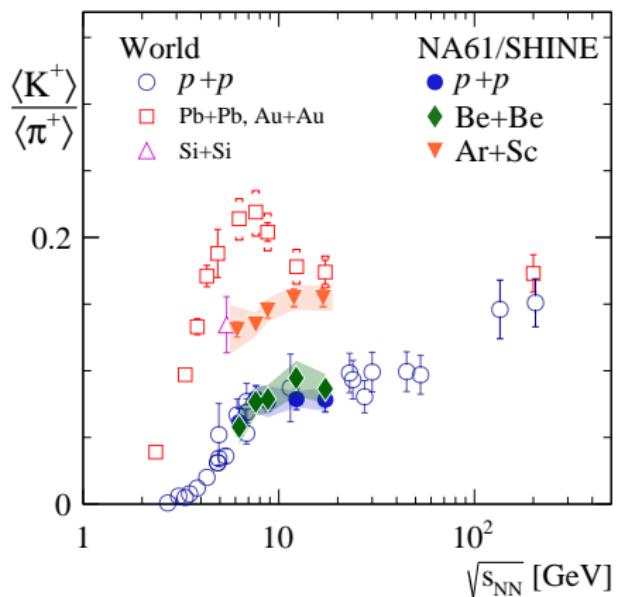


No indications of horn in Ar+Sc collisions.

# Energy dependence of $\langle K^- \rangle / \langle \pi^- \rangle$ and $\langle K^+ \rangle / \langle K^- \rangle$
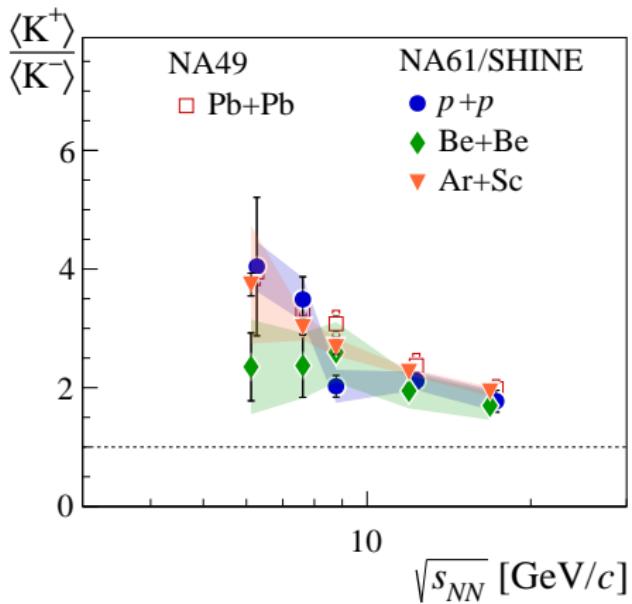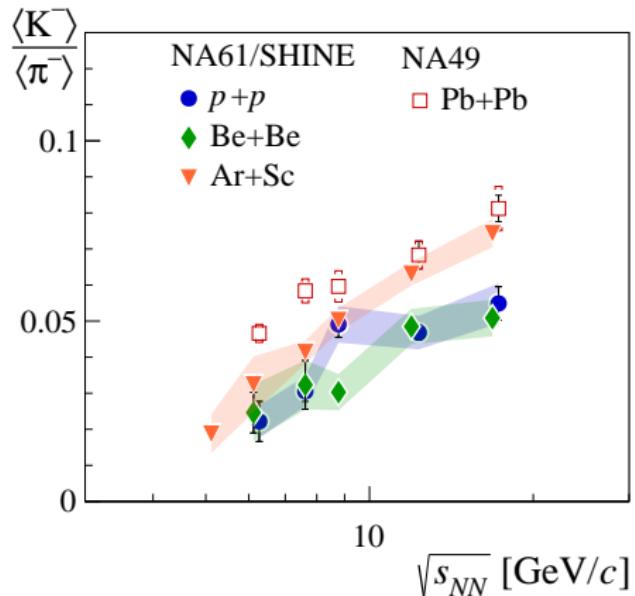


- ▶ The energy dependence looks similar for all systems (considering uncertainties).

Conclusions and summary

# System size dependence – statistical models
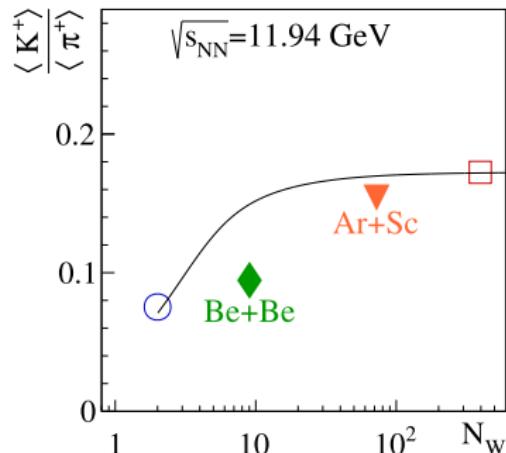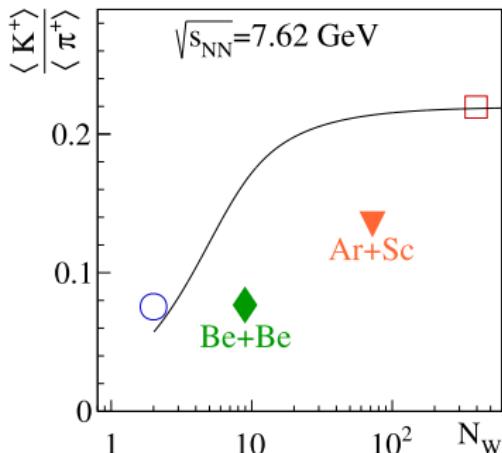


- ▶ Arises due to differences between GC and C formulation.
- ▶ Local conservation of quantum numbers severely reduces the phase space available for particle production.
- ▶ Fails to reproduce measured $K^+/\pi^+$ ratios.

# System size dependence – dynamical models
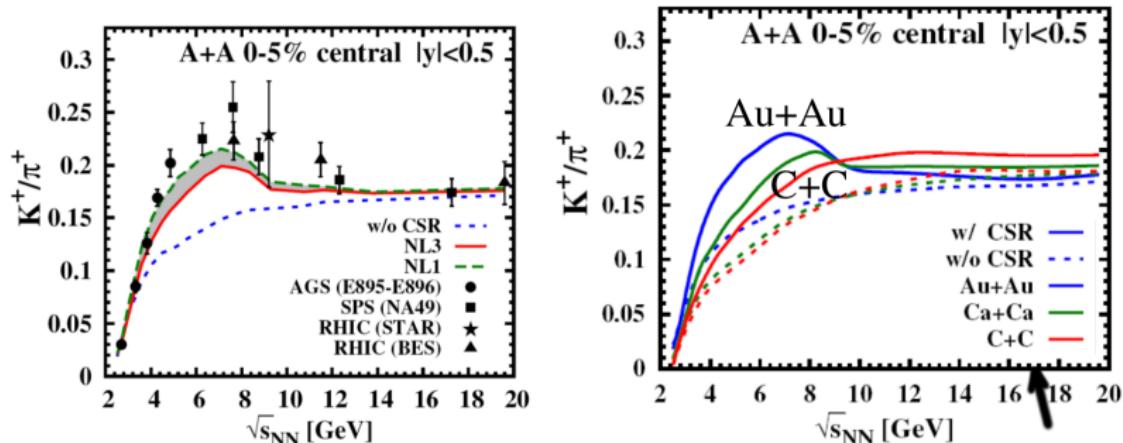


- ▶ PHSD implements the onset of deconfinement.
- ▶ With chiral symmetry restoration – enhanced strangeness production in the confined phase.
- ▶ Predicts increase of strangeness production with system size at low collision energies (<10 GeV) and decrease at high collision energies (>10 GeV).
- ▶ In disagreement with data at high energies.

(Palmese et al. , PRC94 (2016) 044912)

# Proton spectra and the equation of state
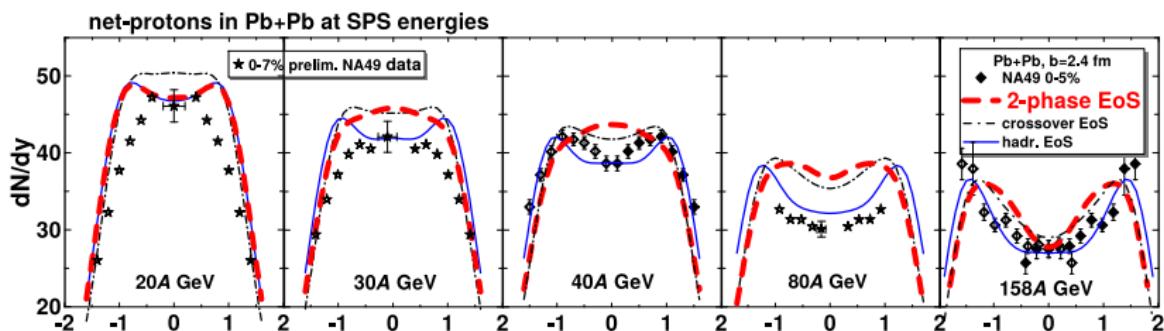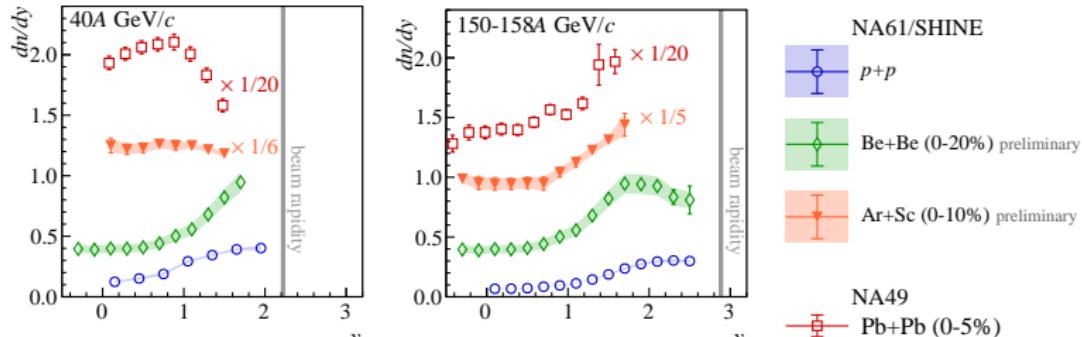


Ivanov, Blaschke; Eur. Phys. J. A (2016) 52: 237

# The onset of fireball
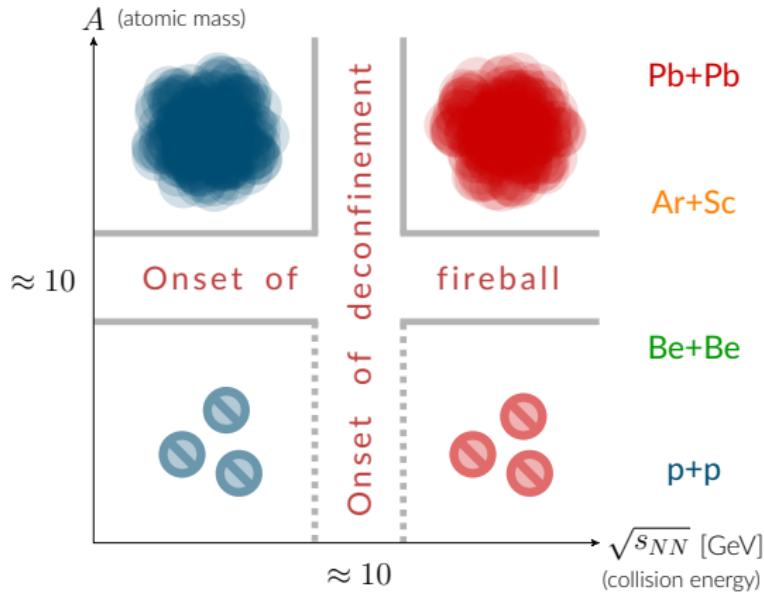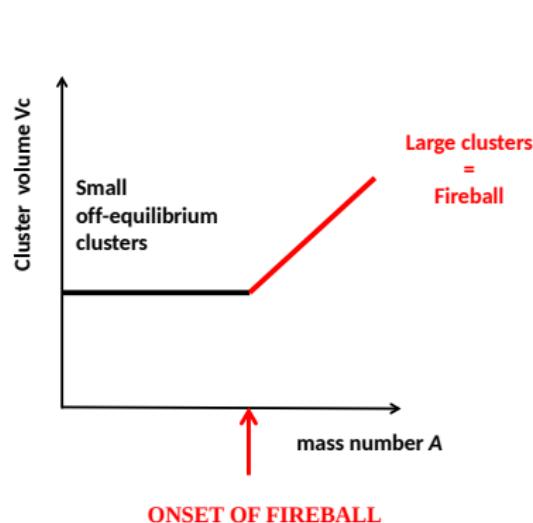


*Onset of fireball*
Beginning of creation of large clusters of strongly interacting matter in nucleus-nucleus collisions with increasing mass number $A$.

# Summary

- The $y$-$p_T$ spectra of charged pion, charged kaons, protons and antiprotons were measured.

- The energy dependence of $\langle K^+\rangle/\langle\pi^+\rangle$ ratio is unlike the non-monotonic behaviour observed in Pb+Pb (and Au+Au) interactions, the ratio monotonically increases with increasing collision energy.

- $\langle K^+\rangle/\langle\pi^+\rangle$ values measured in Ar+Sc collisions are significantly different than at small systems, $p$+$p$ and Be+Be.

- A rapid change of hadron production properties, in $\langle K^+\rangle/\langle\pi^+\rangle$ and $\langle K^-\rangle/\langle\pi^-\rangle$ ratios in particular, that starts when moving from Be+Be to Ar+Sc collisions was observed.

- New measurements of proton and antiproton spectra in Ar+Sc collisions establish an interesting system size dependence when compared against other systems.

- The system size dependence is not yet well understood.

- Ar+Sc appears to be on the boundary between small and large systems.

Backup Slides

# Event and track cuts

Event cuts:

- ▶ Event quality cuts,
- ▶ Target IN,
- ▶ T2 trigger,
- ▶ BPD status,
- ▶ WFA beam (4 $\mu$s),
- ▶ WFA T4 (25 $\mu$s),
- ▶ Fitted main vertex,
- ▶ Perfect vertex fit quality,
- ▶ Fitted vertex position -580 ± 10 cm.
- ▶ PSD quality cuts

Track cuts:

- ▶ track quality cuts,
- ▶ "right-side tracks",
- ▶ >30 clusters in total,
- ▶ >15 clusters in VTPCs
- ▶ $|\phi| < 30°$

# Centrality selection



- ▶ Final results refer to the 10% of Ar+Sc collisions with the lowest value of the forward energy $E_F$.
- ▶ $E_F$ is defined as the total energy of all particles produced in Ar+Sc collisions via strong and electromagnetic processes in the forward momentum region defined by the 3D acceptance map $(p, \theta, \phi)$: *https://edms.cern.ch/document/1867336/1*
- ▶ This procedure allows a precise comparison with predictions of models without any additional information about the NA61/SHINE setup and magnetic field.

# Systematic uncertainty due to centrality selection

▶ $E_F$ – the quantity we would use for selection of *central* events.
  → Cannot be measured directly.

▶ $E_{PSD}$ – the experimentally measured quantity.

Both $E_F$ and $E_{PSD}$ can be obtained in EPOS model.

$$\frac{E_F}{E_{PSD}} \in (1.002, 1.005)$$

More detailed description can be found in Ar+Sc *h*-minus paper:
*cds.cern.ch/record/2749504*

# Asymmetric system $^{40}$Ar+$^{45}$Sc

Two sources of asymmetry:

- $^{40}$Ar projectile is 10% lighter than $^{45}$Sc target.
- Selecting most central events in fact largest number of $N_W$ in $^{40}$Ar projectile is selected (with disregard to $N_W$ in $^{45}$Sc target).

These two contributions introduce biases in opposite directions. $^{40}$Ar+$^{45}$Sc collision system was designed in such a way that these two effects would compensate each other, minimizing the resulting asymmetry.

More detailed analysis can be found in Ar+Sc *h*-minus paper: *cds.cern.ch/record/2749504*

# NA61/SHINE facility

In full glory, including recent updates
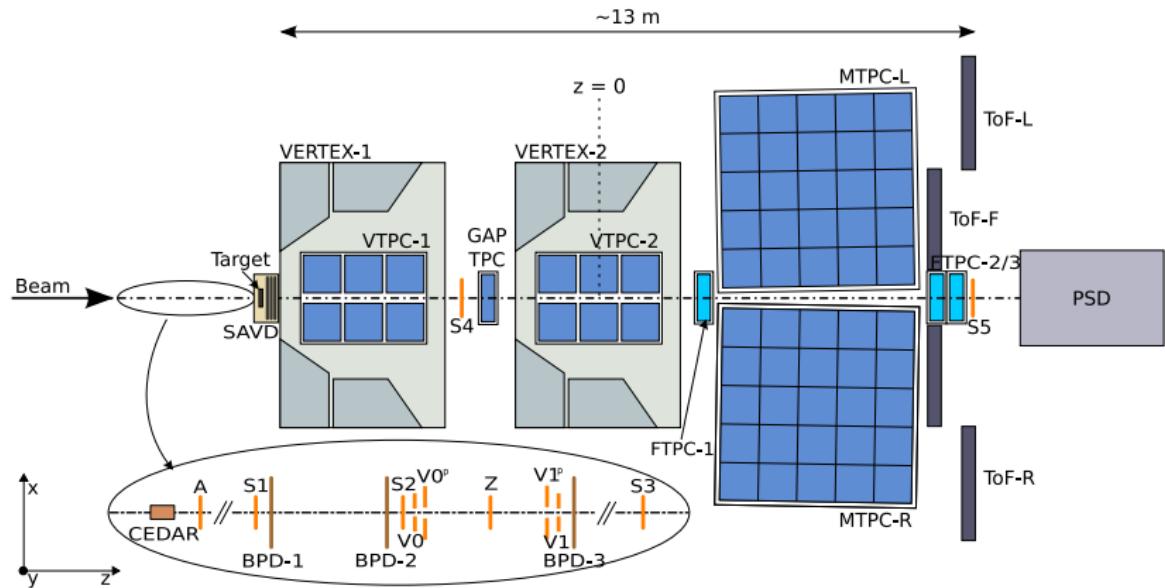
# NA61/SHINE facility

Pre-2018 configuration, showing only components relevant for Ar+Sc
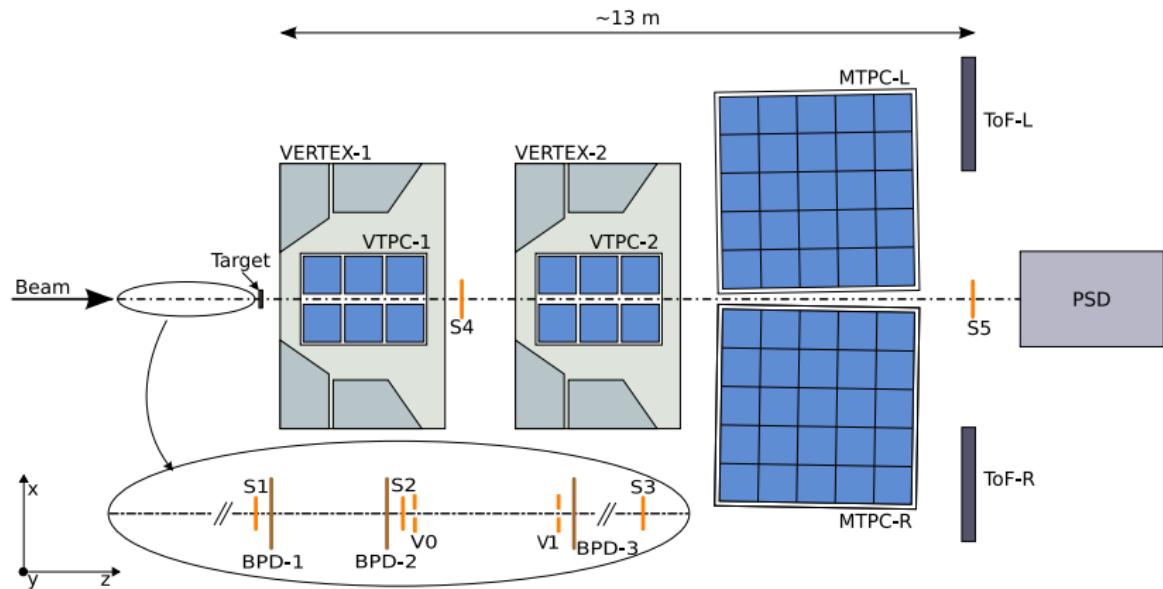
# Model tests

Generated 100k tracks samples.

$x$ at each point is random variable from smeared Vavilov

Truncation at 50% (shaded hist)
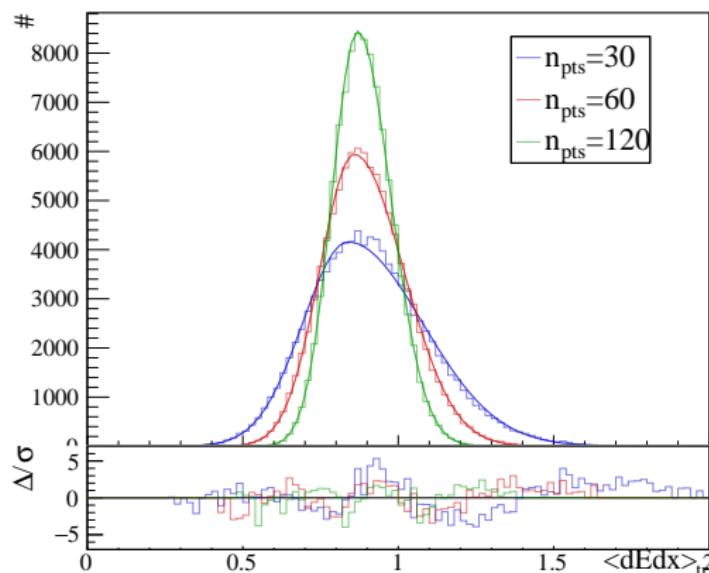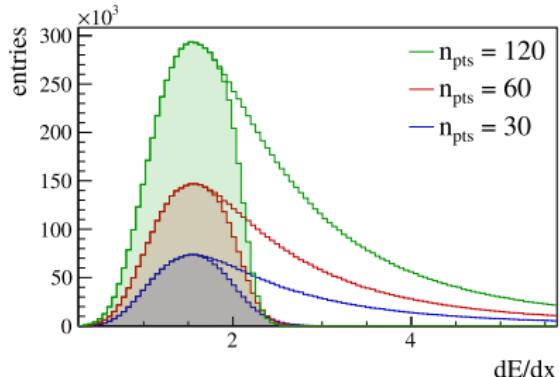


Fitted with asymmetric Gaussian.
Note:
- the width changes
- the maximum moves
- the asymmetry changes

# Model tests



$\sigma$ is not the only parameter dependent on $n_{pts}$!

fitted with:
$$\sigma = \sigma_0 \cdot \sqrt{n_{pts}}$$
$$\delta = \delta_0 \cdot \sqrt{n_{pts}}$$
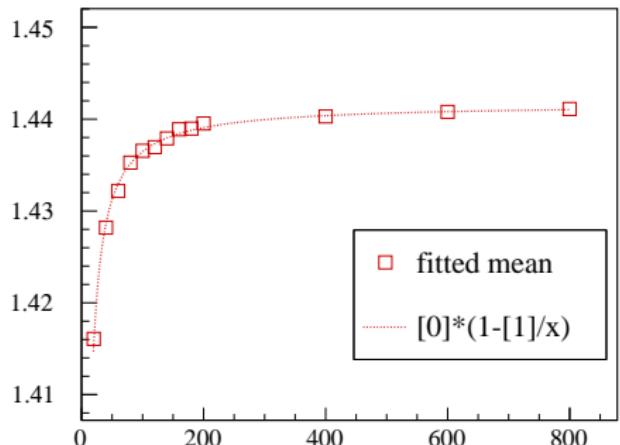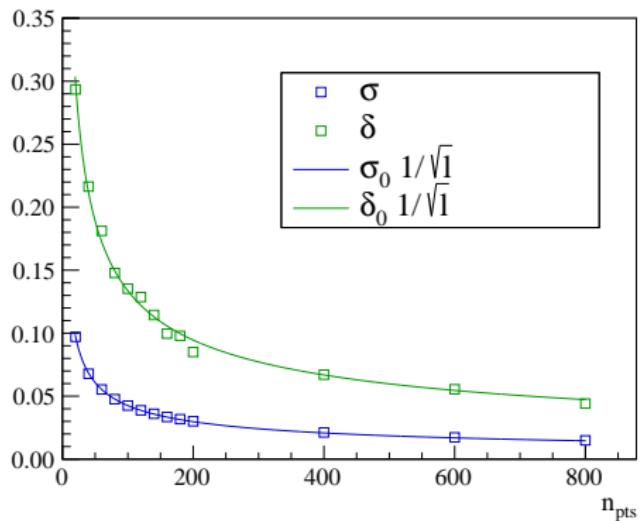


Fitted mean value differs about 5% depending on $n_{pts}$

# Fitting $dE/dx$ distributions

$$\left\langle \frac{dE}{dx} \right\rangle_i = N_i \frac{1}{\sum_l n_l} \sum_l \frac{n_l}{\sqrt{2\pi}\sigma_{i,l}} \exp\left[ -\frac{1}{2} \left( \frac{x - x_i + \frac{2}{\sqrt{2\pi}}\delta\sigma}{(1 \pm \delta)\,\sigma_{i,l}} \right)^2 \right]$$

Problem:

▶ Many separate histograms in bins of $p$ and $p_T$
▶ Many parameters (10-15) in separate models
▶ Some parameters expected to be the same across different bins

Solution – following fit strategy:

1. Fit all $p_T$ bins in a given $p$
   ▶ All parameters free:
     $10 \times n$ bins in $p_T$ and both charges
     + 4 global parameters (relative means $x_i/x_\pi$)
2. Refit with more precision pairs of positive and negative bins at given $p$ and $p_T$ with $x_i/x_\pi$ fixed and $\sigma_0$, $\delta$ as global parameters.

# Identity method with interpolation

$$n[i]^{raw}(y, p_T) = \frac{1}{N_{ev}} \sum_{j=1}^{N_{trk}} W_i(p, p_T, {}^{dE}\!/_{dx})$$

Each track at given $(p, p_T)$ can be assigned with three closest bins of identified particles:

$$(p^{(1)}, p_T{}^{(1)}, W^{(1)}), \quad (p^{(2)}, p_T{}^{(2)}, W^{(2)}), \quad (p^{(3)}, p_T{}^{(3)}, W^{(3)}),$$

$$p^{(1)} = p^{(3)} < p^{(2)}, \quad p_T^{(1)} = p_T^{(2)} < p_T^{(3)}$$

Interpolation in $p$:

$$W^{(1\text{-}2)} = W^{(1)} + (p - p^{(1)}) \frac{W^{(2)} - W^{(1)}}{p^{(2)} - p^{(1)}}$$

Interpolation in $p_T$:

$$W^{(1\text{-}2\text{-}3)} = W^{(3)} + (p_T - p_T{}^{(1)}) \frac{W^{(12)} - W^{(3)}}{p_T{}^{(3)} - p_T{}^{(1)}}$$

$W^{(1\text{-}2\text{-}3)} \equiv W_i(p, p_T, {}^{dE}\!/_{dx})$ are probabilities (weights) assigned in the identity method.
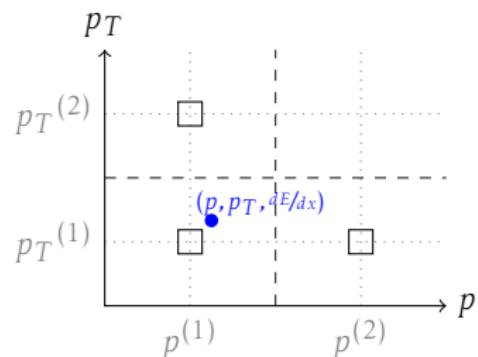
# Models of strangeness production

There are multiple approaches to describe the strangeness production in HIC.
I want to briefly introduce some of them:

- ▶ Statistical Models:
    - ▶ Hadron Resonance Gas
    - ▶ Statistical Hadronization Model
    - ▶ Statistical Model of Early Stage ◂

- ▶ Dynamical Models:
    - ▶ Rafelski-Müller toy model
    - ▶ Parton-Hadron String Dynamics ◂

include
deconfinement
explicitly

# Hadron Resonance Gas

$\rightarrow$ Assumption of chemical equilibrium.
Density of particle species $i$:

$$n_i(\mu, T) = \frac{N_i}{V} = -\frac{T}{V}\frac{\partial ln Z_i}{\partial \mu} = \frac{g_i}{2\pi^2}\int \frac{p^2 dp}{e^{\frac{E_i - \mu_i}{T}} \pm 1}, \quad \mu_i = \mu_B B_i + \mu_S S_i + \mu_{I_3} I_{3,i}$$

Chemical potentials $\mu_i$ constrained by conservation laws:

baryon number:
$$V\sum_i n_i B_i = Z + N \rightarrow \mu_B$$

strangeness:
$$V\sum_i n_i S_i = 0 \rightarrow \mu_s$$

charge:
$$V\sum_i n_i I_{3,i} = \frac{Z - N}{2} \rightarrow \mu_{I_{3,i}}$$

3 equations,
5 unknowns
$\downarrow$
2 free
parameters

Two free parameters $(T, \mu_B)$ are fitted to experimental data on particle yields.

# Particle yields – input to HRG model
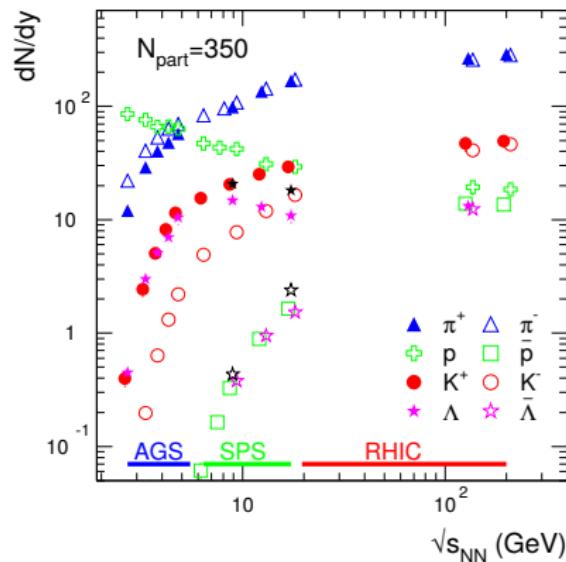


The energy dependence of experimental hadron yields at mid-rapidity for various species produced in central nucleus-nucleus collisions.

(Andronic, Braun-Munzinger, Stachel; Nucl.Phys.A772:167-199,2006)

# Hadron Resonance Gas
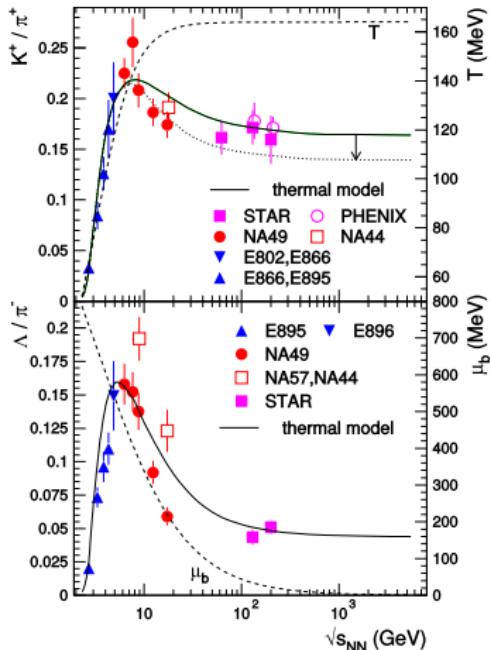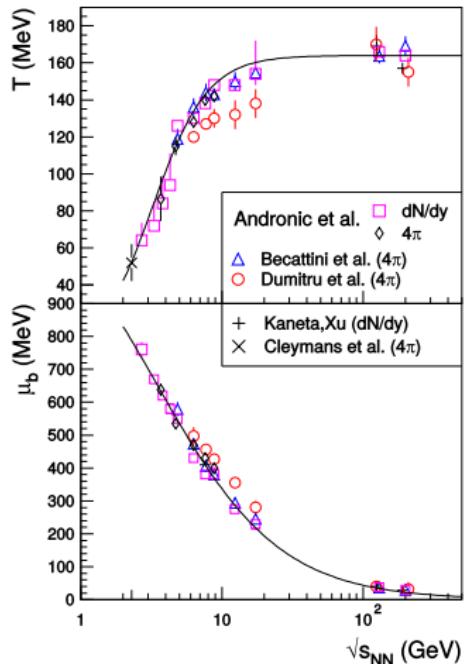


(Andronic, Braun-Munzinger, Stachel; Nucl.Phys. A834 (2010) 237C-240C)

# Statistical Hadronization – $\gamma_s$, $\gamma_q$

Results on strangess in HRG were not satisfactory.

Parameter of "phase-space occupancy" $\gamma_s$ introduced to improve the fits:

$$\langle \frac{N_s}{V} \rangle = \langle \rho_s \rangle = \int \frac{d^3p}{(2\pi)^3} \frac{1}{\lambda_s^{-1} \gamma_s^{-1} e^{E(p)/T} + 1}, \quad \langle \frac{N_{\bar{s}}}{V} \rangle = \langle \rho_{\bar{s}} \rangle = \int \frac{d^3p}{(2\pi)^3} \frac{1}{\lambda_s \gamma_s^{-1} e^{E(p)/T} + 1}$$

Due to larger mass of $s$ quark it requires more time to saturate and so it doesn't reach equilibrium value.
$\rightarrow \gamma_s < 1$ at lower collision energies (AGS, SPS).
$\rightarrow \gamma_s = 1$ at higher energies (from RHIC).

# Statistical Hadronization – $\gamma_s$, $\gamma_q$

Results on strangess in HRG were not satisfactory.

Parameter of "phase-space occupancy" $\gamma_s$ introduced to improve the fits:

$$\langle \frac{N_s}{V} \rangle = \langle \rho_s \rangle = \int \frac{d^3p}{(2\pi)^3} \frac{1}{\lambda_s^{-1} \gamma_s^{-1} e^{E(p)/T} + 1}, \quad \langle \frac{N_{\bar{s}}}{V} \rangle = \langle \rho_{\bar{s}} \rangle = \int \frac{d^3p}{(2\pi)^3} \frac{1}{\lambda_s \gamma_s^{-1} e^{E(p)/T} + 1}$$

Due to larger mass of $s$ quark it requires more time to saturate and so it doesn't reach equilibrium value.
$\rightarrow \gamma_s < 1$ at lower collision energies (AGS, SPS).
$\rightarrow \gamma_s = 1$ at higher energies (from RHIC).

Later on $\gamma_q$ was introduced to tune the fits for $u, d$ quarks.

# Statistical Hadronization – $\gamma_s$, $\gamma_q$
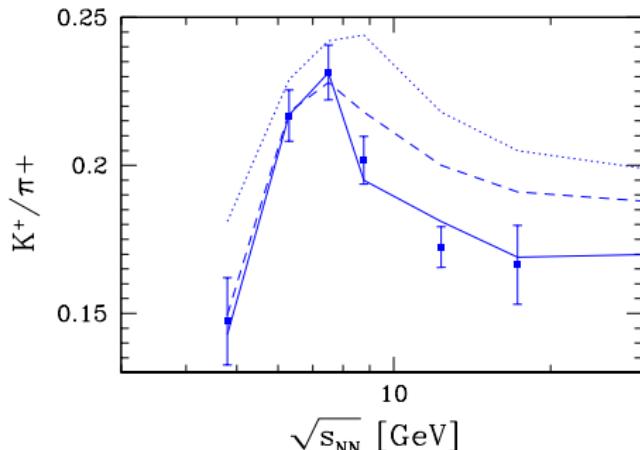


dotted: $\gamma_q, \gamma_s = 1$
dashed: $\gamma_q = 1, \gamma_s < 1$
solid: $\gamma_q, \gamma_s < 1$

but is it still a statistical model?

# Dynamical Approach by Rafelski-Müller

strangeness production <u>in confined matter</u>

$$N + N \rightarrow N + Y + K$$

$$\pi + N \rightarrow K + Y \qquad\qquad \pi + \overline{N} \rightarrow \overline{K} + \overline{Y}$$
$$\pi + Y \rightarrow \Xi + K \qquad\qquad \pi + \overline{Y} \rightarrow \overline{\Xi} + \overline{K}$$
$$\pi + \Xi \rightarrow \Omega + K \qquad\qquad \pi + \overline{\Xi} \rightarrow \overline{\Omega} + \overline{K}$$
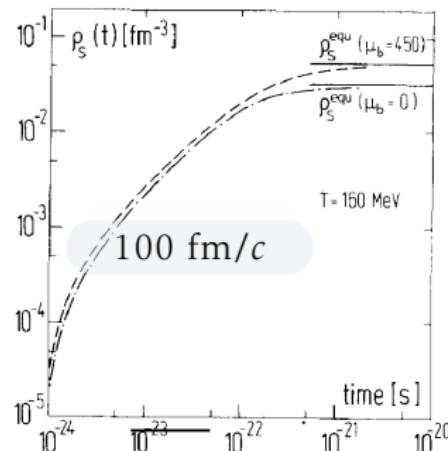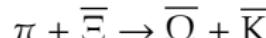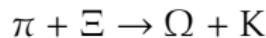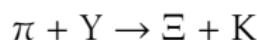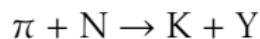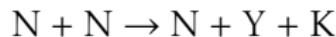
strangeness production <u>in QGP</u>





(Rafelski, Müller, Phys. Rev. Lett. 48 (1982) 1066)
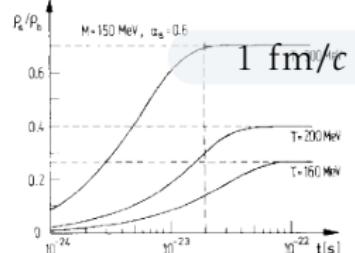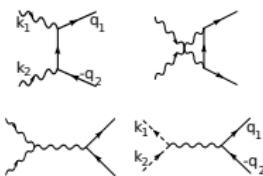
# Rafelski-Müller Dynamical Approach
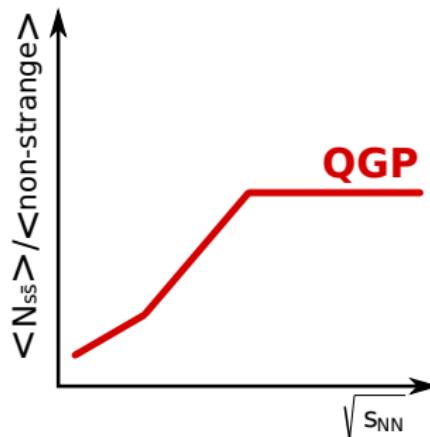


- ▶ Equilibrium value reached in QGP ← fast strangeness production.
- ▶ No enhancement in the confined phase ← slow strangeness production in whole hadronic region.
- ▶ Deconfinement happens in the collisions of heavy ions, but not in p+p interactions.
  → explanation for system size dependence (*A+A* vs *p+p*).

# PHSD model with & without Chiral Symmetry Restoration
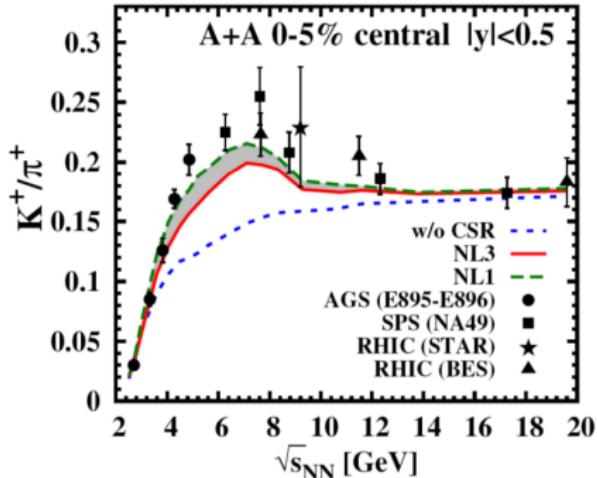
- ▶ Implements the onset of deconfinement.
- ▶ <u>Without CSR</u> – prediction of PHSD qualitatively resembles predictions of the Rafelski-Müller model.
- ▶ <u>With CSR</u> – enhanced strangeness production in the confined phase.
  The strange quark mass used in the string decay Schwinger-formula in assumed to decrease with energy density, while still in the confined phase.

(Palmese et al. , PRC94 (2016) 044912)    19/41

# Collision energy dependence of strangeness production

"horn" plot
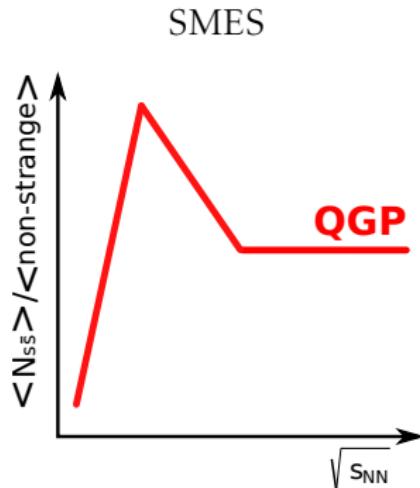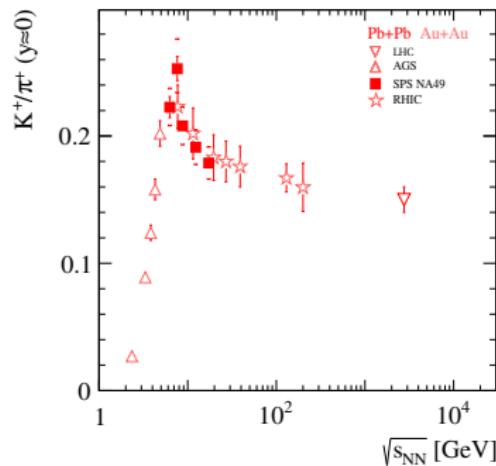


- Qualitatively, heavy-ion data follows dependence predicted by SMES.

# Before NA61/SHINE
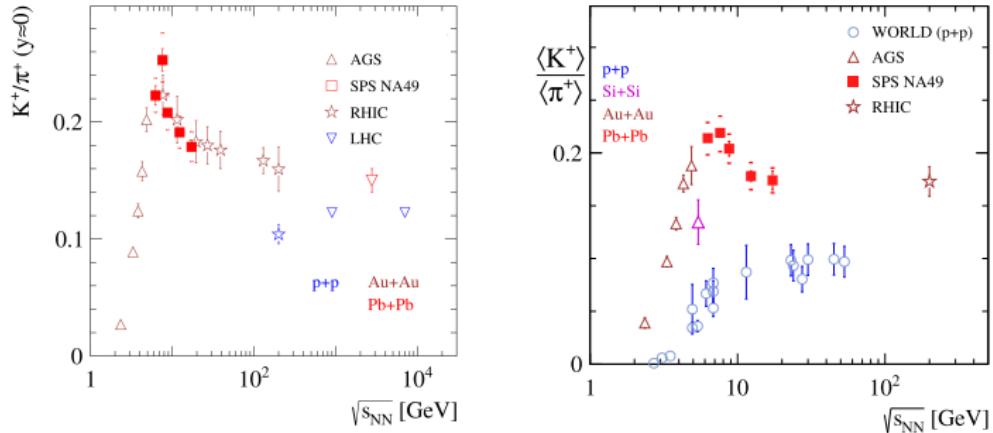


- ▶ No precise baseline of p+p collisions.
- ▶ No data on system size dependence of particle production at SPS energies – vicinity of the onset of deconfinement.

# The onset of deconfinement – predictions of SMES
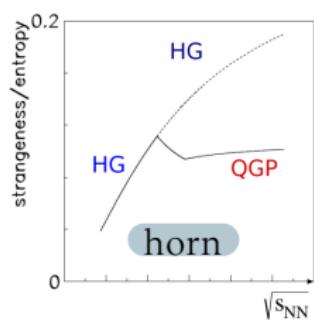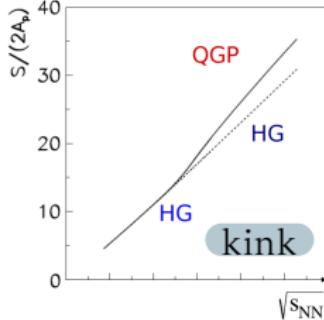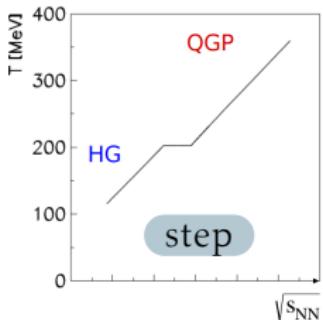


Plateau in "temperature" dependence on $\sqrt{s_{NN}}$
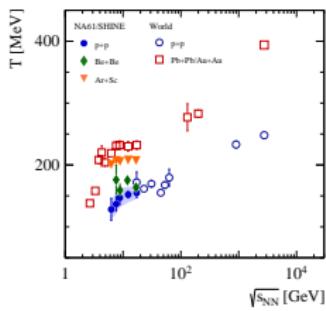
Enhancement of entropy production in QGP phase
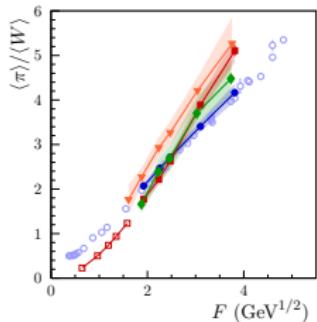
Suppresion of strangeness production in QGP phase
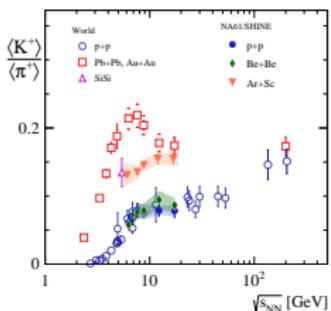
Signatures of PT happen all at the same $\sqrt{s_{NN}}$.

# $\pi^-$ in d$E$/d$x$ vs $h$-minus validation
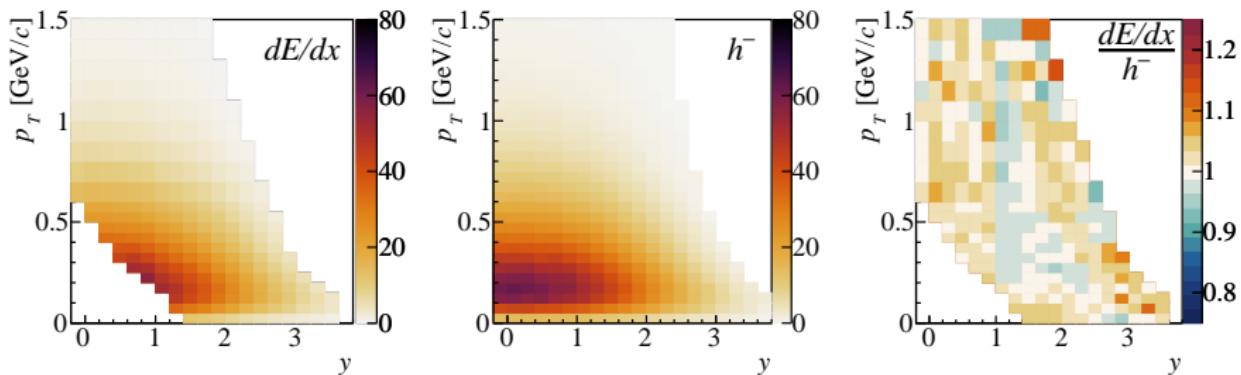


$\mathrm{d}^2n/\mathrm{d}y,\mathrm{d}p_T$ $[(\mathrm{GeV}/c)^{-1}]$ spectrum of $\pi^-$ at $150A$ GeV/$c$ using:

▶ Left: d$E$/d$x$ method.

▶ Middle: $h$-minus method

Right: ratio of results from these two methods.
Discrepancies rarely exceed 2.5%.

$\pi^-$ vs $\pi^+$

| $p_{\text{beam}}$ [GeV/$c$] | 13$A$ | 19$A$ | 30$A$ | 40$A$ | 75$A$ | 150$A$ |
|---|---|---|---|---|---|---|
| $\pi^+/\pi^-$ EPOS | 0.954 | 0.961 | 0.969 | 0.972 | 0.978 | 0.983 |
| $\pi^+/\pi^-$ in $dE/dx$ acc. | 0.884 | 0.949 | 0.933 | 0.929 | 0.952 | 0.975 |

- $dE/dx$ acceptance shrinks at lower collision energies.
- $\pi^+/\pi^-$ is close to one both in EPOS and data.

Following approximation:

$$\langle \pi^+ \rangle \approx \langle \pi^- \rangle$$

was used to obtain $\langle \pi^+ \rangle$ yield.

# Charged pions in EPOS
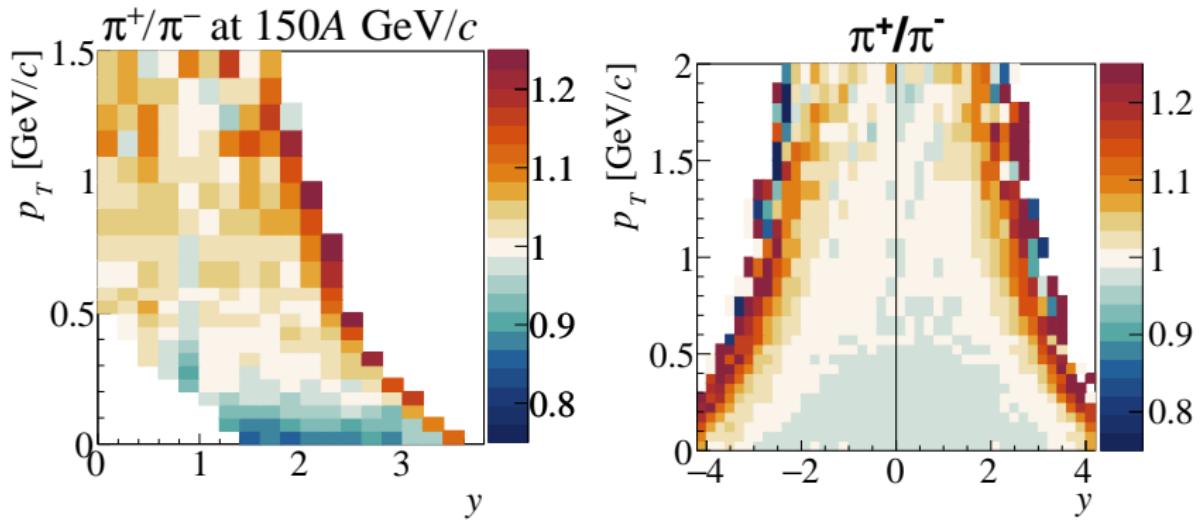


$\pi^+/\pi^-$ at 150$A$ GeV/$c$

Note that the dip in $\pi^+/\pi^-$ ratio at small $p_T$ is an effect of electromagnetic interactions and it is not reproduced by used model.

# Kaon spectra

Obtaining $4\pi$ acceptance, extrapolation

▶ $p_T$ spectra

$p_T$ spectra of kaons are fitted with following function:

$$\frac{1}{p_T}\frac{d^2}{dp_T\, py} = \frac{A}{T\,(m_K + T)} \cdot e^{-(m_T - m_K)/T}$$

Fit range [0.0;1.5] GeV/$c$ (or first/last bin above zero).
The value of $dn/dy$ is taken as the sum of the measurement points in $p_T$
distribution and the integral of fit function outside of the acceptance region.

▶ $y$ spectra

Fitting $dn/dy$ distribution:

$$f_{\text{fit}}(y) = \frac{A}{\sigma_0\sqrt{2\pi}}\exp\left(\frac{-(y - y_0)^2}{2\sigma_0^2}\right) + \frac{A}{\sigma_0\sqrt{2\pi}}\exp\left(\frac{-(y + y_0)^2}{2\sigma_0^2}\right)$$

Symmetry of backward and forward rapidity is assumed (for now).
$A$, $y_0$ and $\sigma_0$ are free parameters.
Mean multiplicity is taken as the sum of the measured points in $y$
distribution and the integral of fit function outside of the acceptance region.

# System size dependence
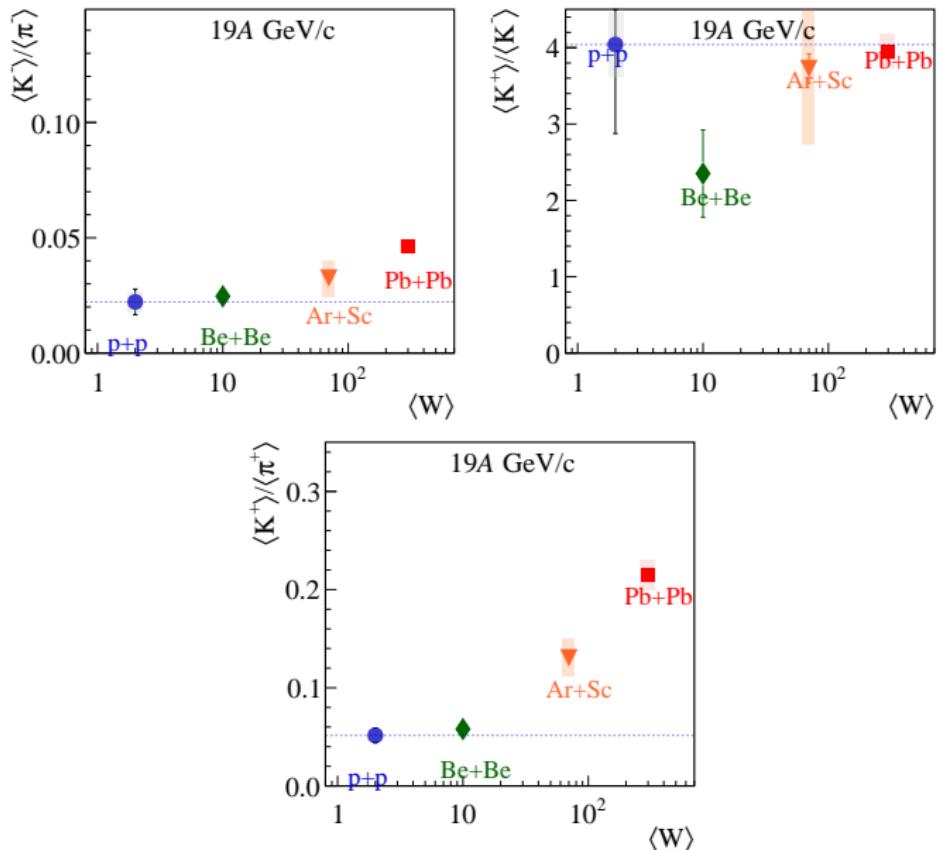
# System size dependence
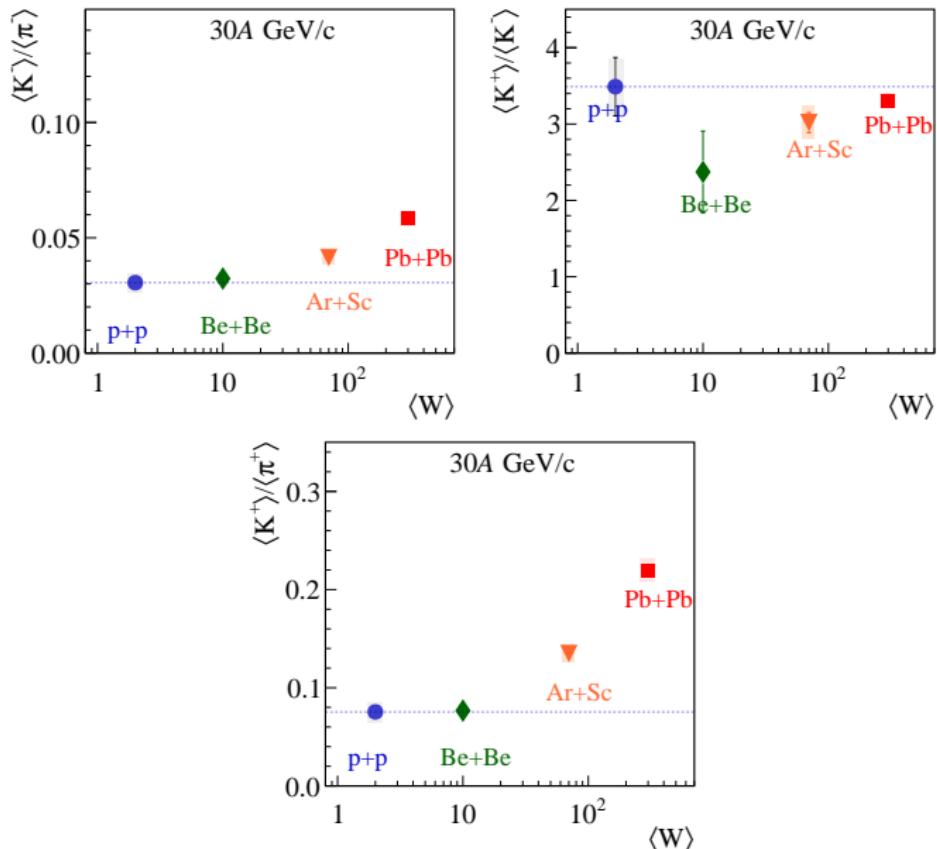
# System size dependence
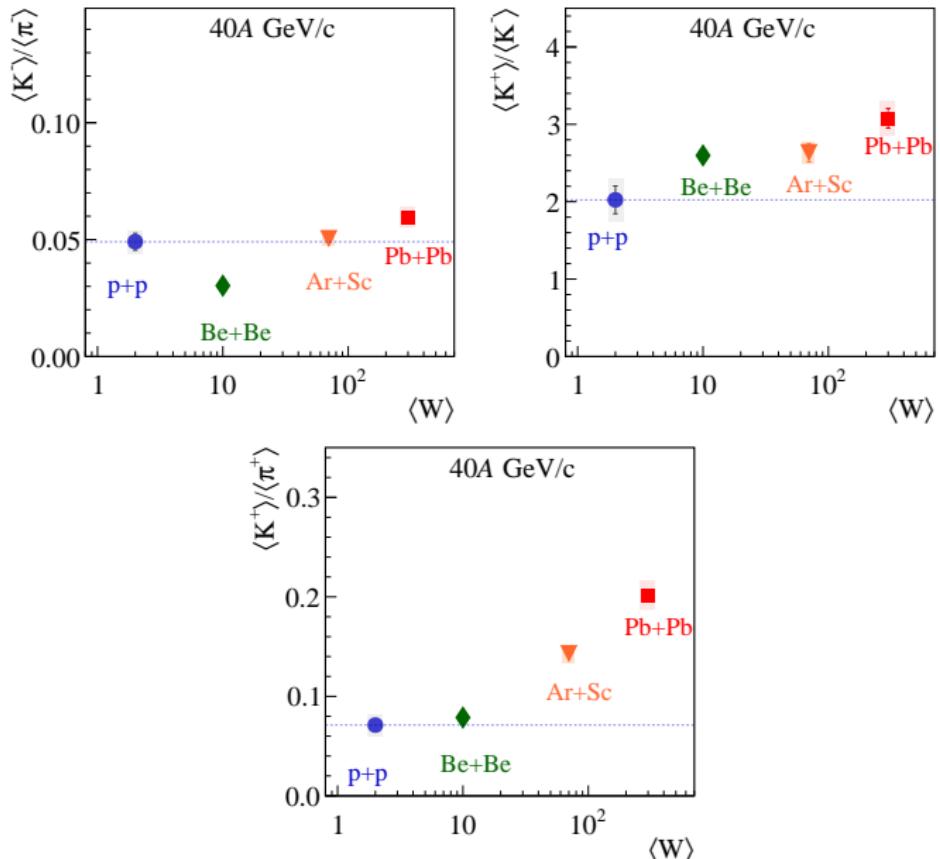
# System size dependence
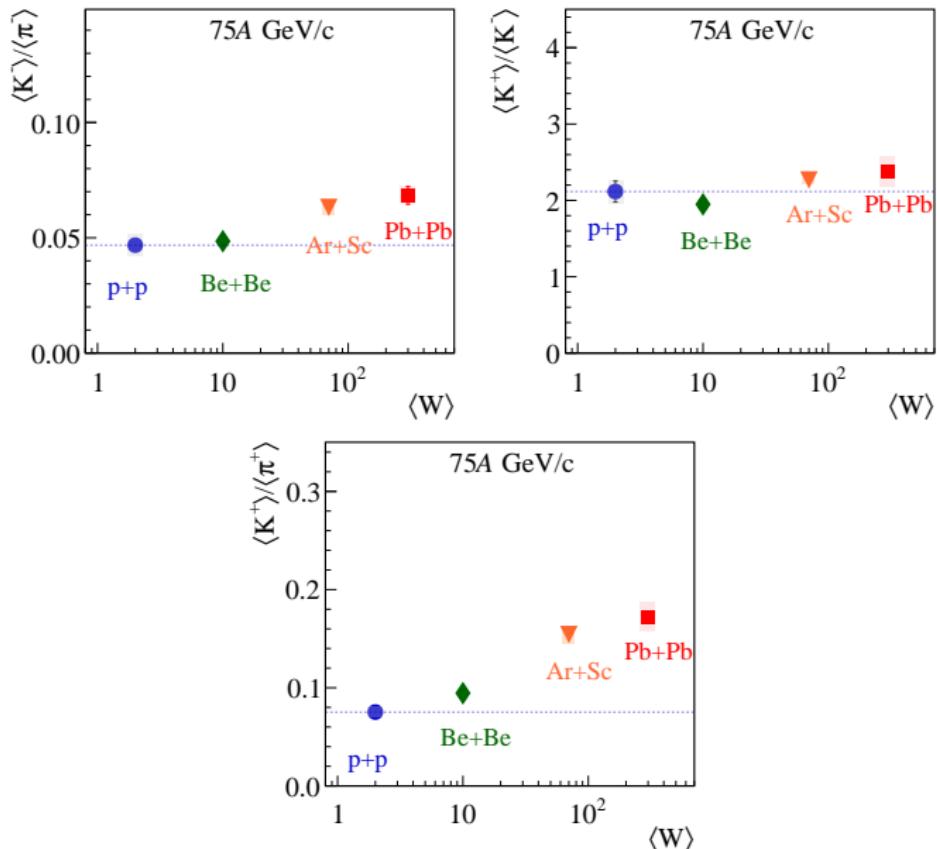
# System size dependence
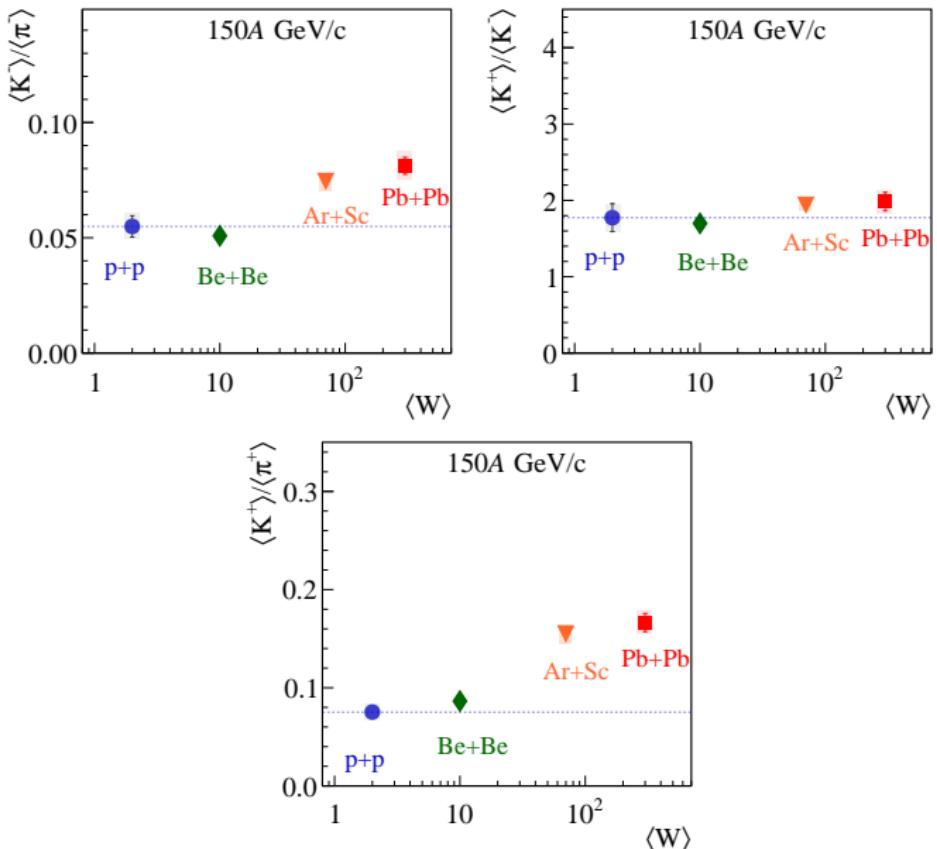
# Inverse slope parameter $T$
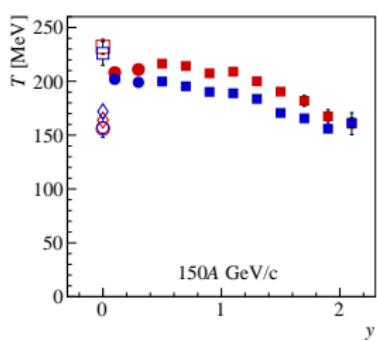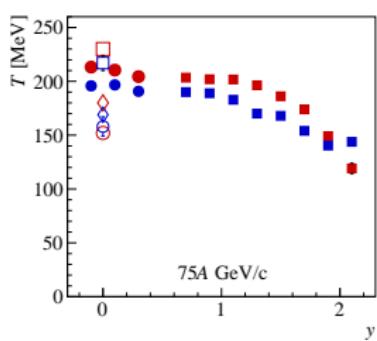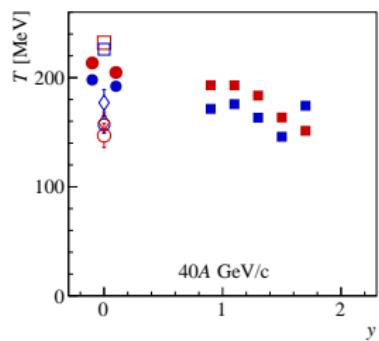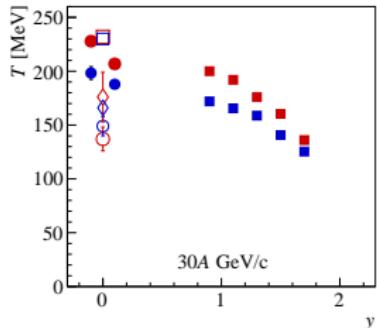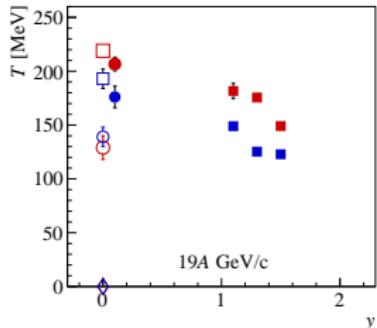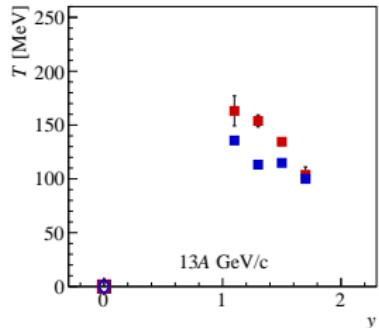
0-10% most central events, no systematic uncertainty calculated

# Kaon rapidity spectra



$Ar + Sc \rightarrow K^+ + X$

$Ar + Sc \rightarrow K^- + X$
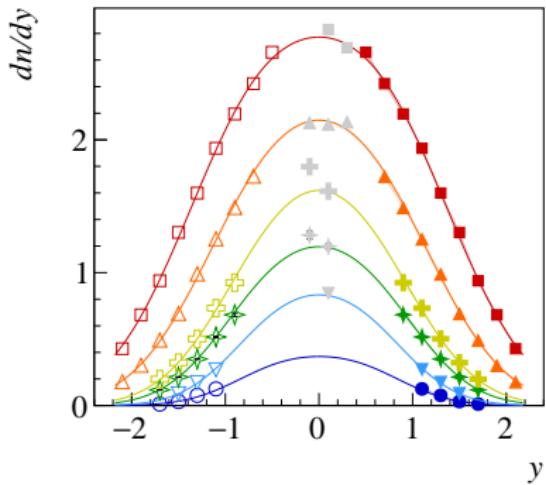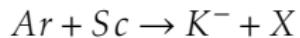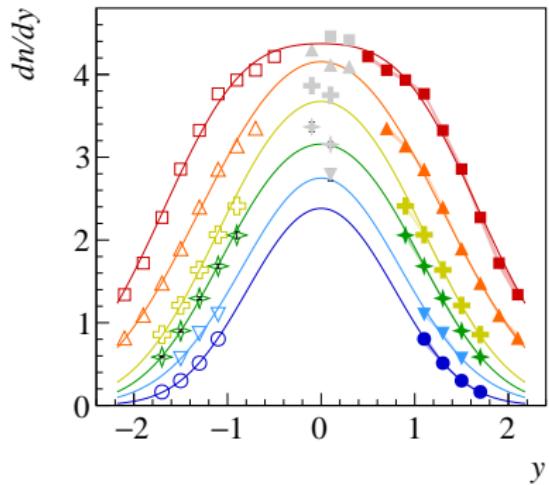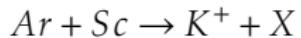
0-10% most central events
Gray points are preliminary results of $tof\text{-}dE/dx$ analysis by Piotr.

# Kaon rapidity spectra fitting
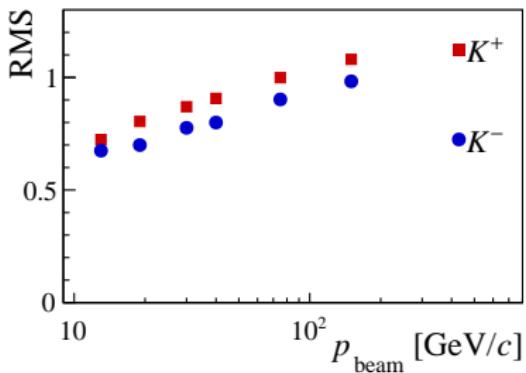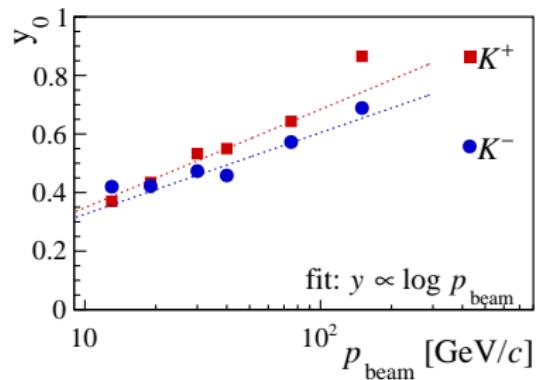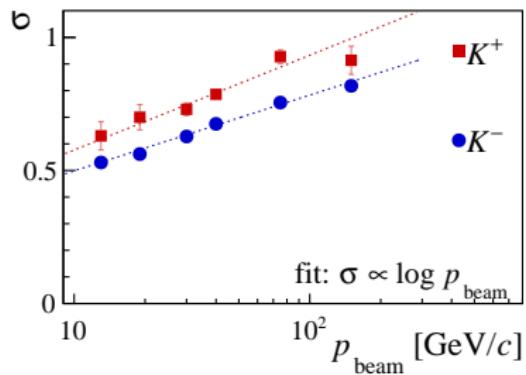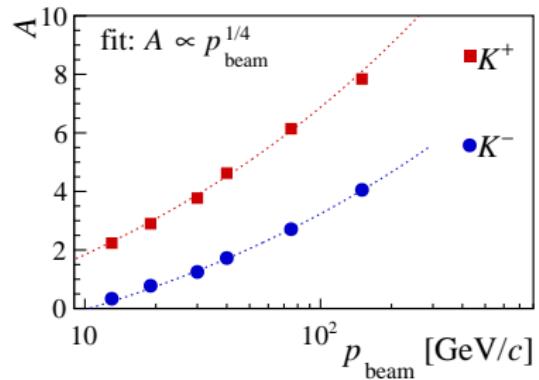
# Kaon spectra
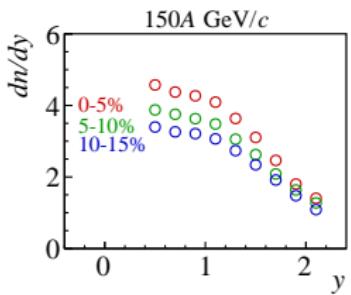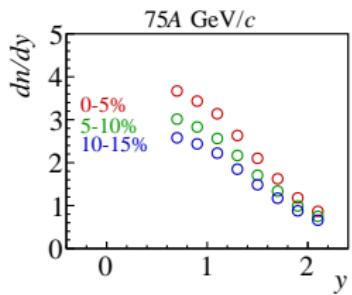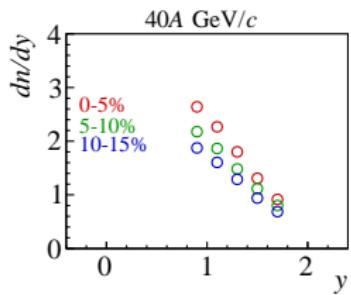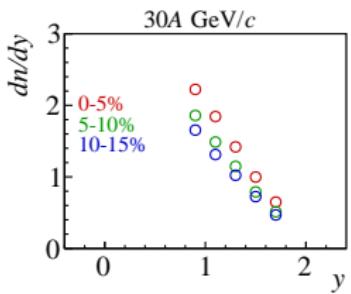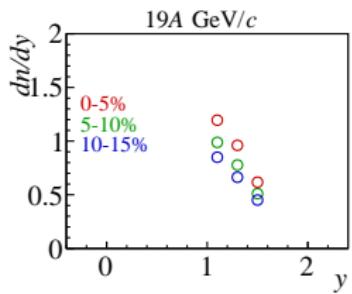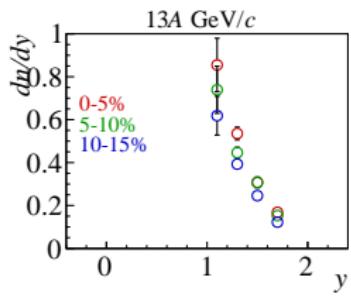
$Ar + Sc \rightarrow K^+ + X$



3 bins of centrality: 0-5%, 5-10% and 10-15%.
Note that some of these (10-15% in particular) can be subject to trigger bias, details here.

# Kaon spectra
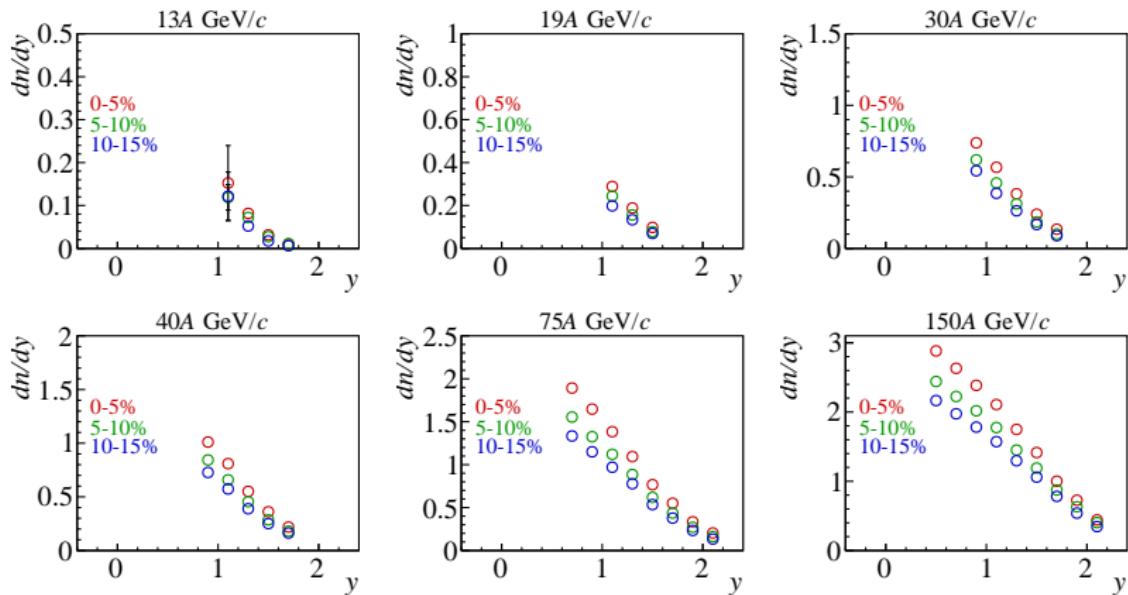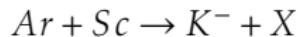
$Ar + Sc \to K^- + X$



3 bins of centrality: 0-5%, 5-10% and 10-15%.
Note that some of these (10-15% in particular) can be subject to trigger bias, details <u>here</u>.

# Proton spectra

$Ar + Sc \rightarrow p + X$
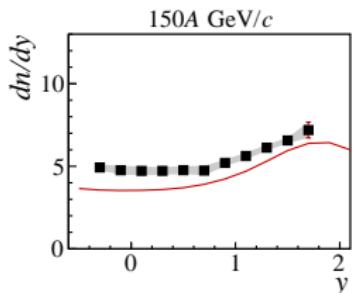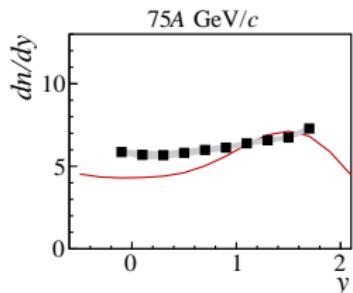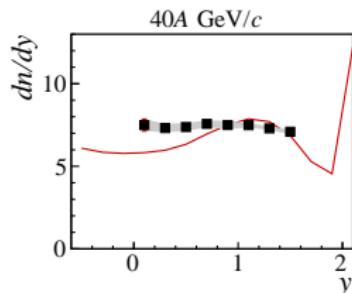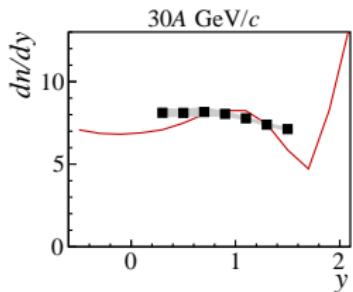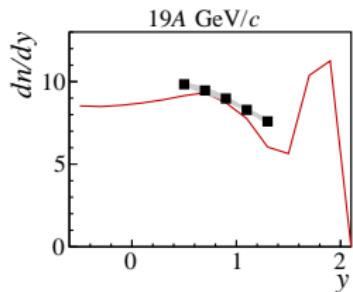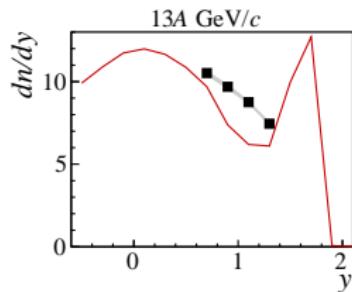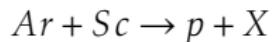


0-10% most central events
EPOS (red line) describes the spectra surprisingly well.

# Proton spectra
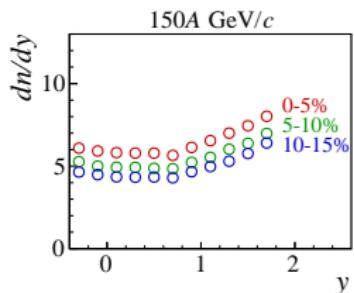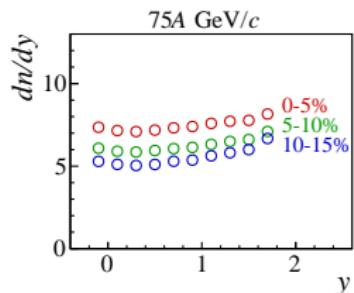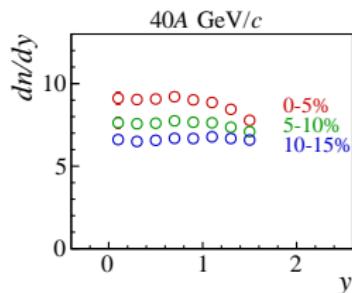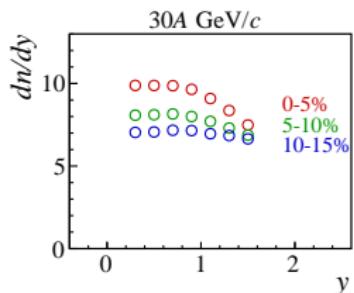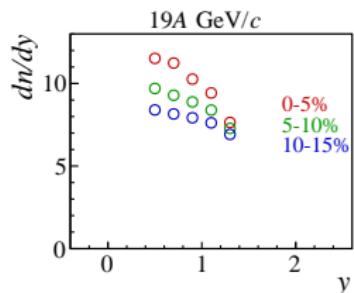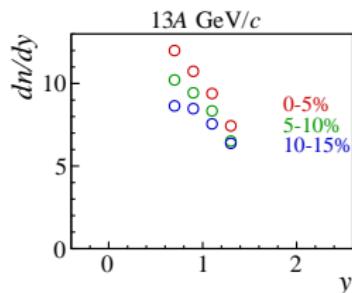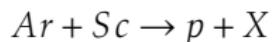
$Ar + Sc \rightarrow p + X$



3 bins of centrality: 0-5%, 5-10% and 10-15%.
Note that some of these (10-15% in particular) can be subject to trigger bias.

# Antiproton spectra

$Ar + Sc \rightarrow \bar{p} + X$
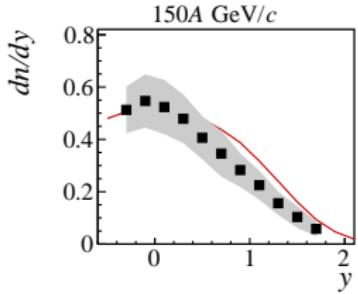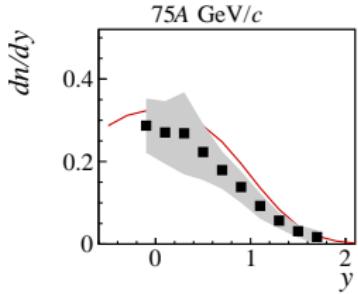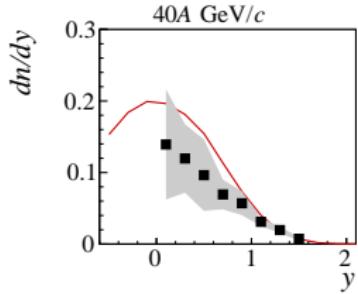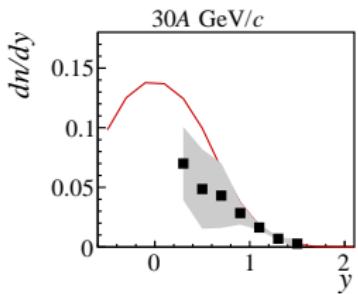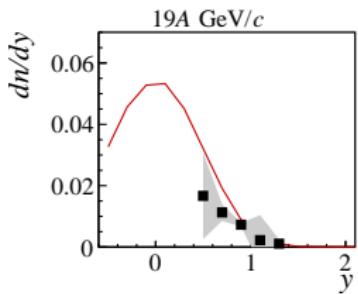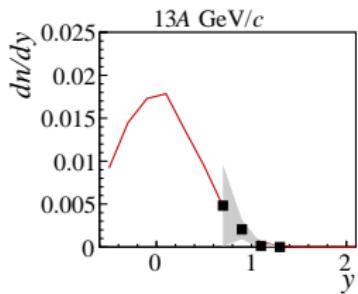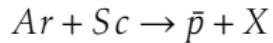


0-10% most central events

# Antiproton spectra
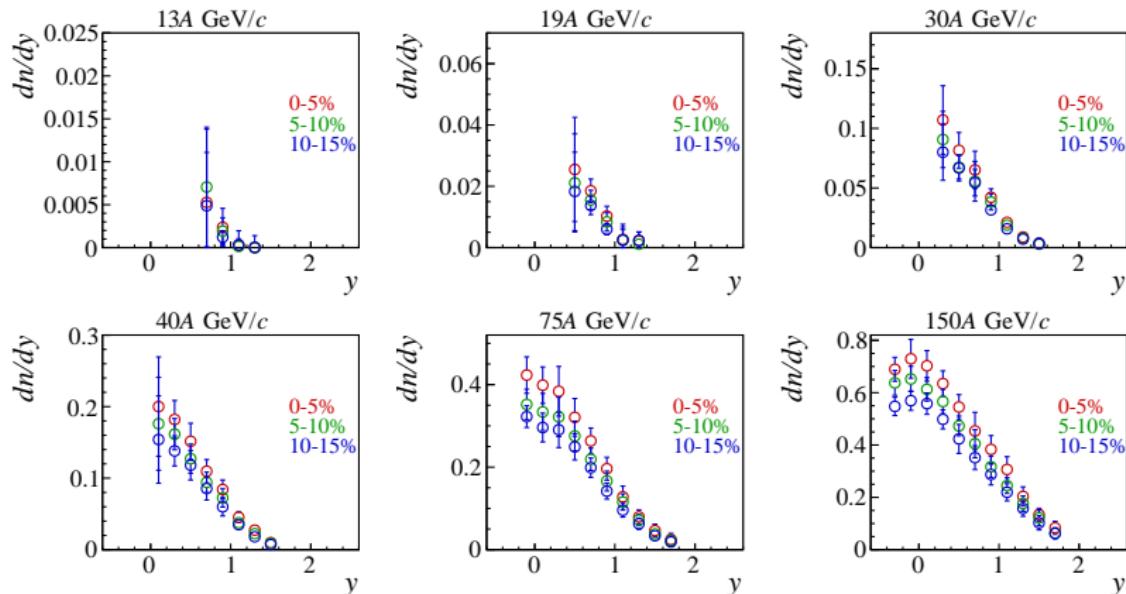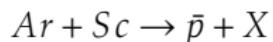
$Ar + Sc \rightarrow \bar{p} + X$



3 bins of centrality: 0-5%, 5-10% and 10-15%.
Note that some of these (10-15% in particular) can be subject to trigger bias.

# Comparison with other measured systems